Available online at www.sciencedirect.com
ScienceDirect
Geochimica et Cosmochimica Acta 72 (2008) 4254–4277
Geochimica et Cosmochimica Acta
www.elsevier.com/locate/gca

Geochemistry of the dissolved load of the Changjiang Basin rivers: Anthropogenic impacts and chemical weathering

B. Chetelat *, C.-Q. Liu *, Z.Q. Zhao, Q.L. Wang, S.L. Li, J. Li, B.L. Wang

State Key Laboratory of Environmental Geochemistry, Institute of Geochemistry, CAS, 46 Guanshui Road, 55002 Guiyang, PR China

Received 12 February 2008; accepted in revised form 10 June 2008; available online 25 June 2008

Abstract

This study focuses on the chemical and Sr isotopic compositions of the dissolved load of the rivers of the Changjiang Basin, one of the largest riverine systems in the world. Water samples were collected in August 2006 from the main tributaries and the main Changjiang channel. The chemical and isotopic analyses indicated that four major reservoirs (carbonates, silicates, evaporites and agriculture/urban effluents) contribute to the total dissolved solutes. The overall chemical weathering (carbonate and silicate) rate for the Changjiang is approximately 40 ton/km^2/year or 19 mm/kyr, similar to that of the Ganges–Brahmaputra system, and the basin is characterized by carbonate and silicate weathering rates ranging from 17 to 56 ton/km^2/year and from 0.7 to 7.1 ton/km^2/year, respectively. In the lower reach of the Changjiang main channel, the weathering rates are estimated to be 36 and 2.2 ton/km^2/year for carbonates and silicates, respectively. It appears that sulphuric acid may dominate chemical weathering reactions for some sub-basins. The budgets of CO_2 consumption are estimated to be 646×10^9 and 191×10^9 mol/year by carbonate and silicate weathering, respectively. The contribution of the anthropogenic inputs to the cationic TDS of the Changjiang is estimated to be 15–20% for the most downstream stations. Our study suggested that the Changjiang is strongly impacted by human activities and is very sensitive to the change of land use.

1. INTRODUCTION

Under the influence of meteoric water and other factors like glaciers, wind and vegetation, continents are continuously subjected to erosion. Rainwater and surface water interact with minerals of the Earth's surface, resulting in the dissolution of primary minerals and the production of secondary clays and iron or aluminium oxides that accumulate in soils. Erosion is not only important at a geological time scale, responsible for the landscape evolution but also a key process in the soil formation and stability. Therefore, erosion has important consequences for agriculture and human sustainable development.

The study of the dissolved load of rivers provides information on chemical erosion processes (Gaillardet et al., 1999b; Dalai et al., 2002; Wu et al., 2005 and references therein), in particular on velocity of soil formation. The study of sediments (in suspension or at the river bed) is important for understanding the physical processes, in particular the rate of soil erosion (natural or not). Based on chemical mass balances between the solid phase and the dissolved load of rivers (Gaillardet et al., 1999a; Dosseto et al., 2008 and references therein), geo-scientists are able to deduce fundamental information about the Earth's surface dynamics. For example, chemical weathering of silicates is the dominant long-term sink for atmospheric CO_2 and thus the dominant regulator of the green-house effect over geological time-scales (Berner et al., 1983; Raymo et al., 1988; Godderis and Francois, 1995; Dessert et al., 2003; Godderis et al., 2003). Hence, quantifying chemical weathering rates is essential for understanding Earth's long-term climatic evolution.

The Changjiang basin is particularly well suited for quantifying erosion processes because it is one of the world largest rivers and averages erosion processes over a huge

* Corresponding authors.
E-mail addresses: benjamin@vip.gyig.ac.cn (B. Chetelat), liucongqiang@vip.skleg.ac.cn (C.-Q. Liu).

0016-7037/$ - see front matter © 2008 Elsevier Ltd. All rights reserved.
doi:10.1016/j.gca.2008.06.013

surface of the Earth (1.81×10^6 km^2, 19% of China). The Upper Changjiang drains the Tibetan Plateau, and provides a better understanding of the way and rate at which the erosion of the Tibetan plateau proceeds. In its lower part, the Changjiang drains one of the most populated areas of the world and is affected by the Three Gorges Dam (TGD), the biggest dam in the world. The Changijiang integrates anthropogenic pollution over a large surface area. Better knowledge of its chemical composition and solid transport is critical to understanding how human activities have changed the river chemistry and soil erosion. The Earth is experiencing a unique global climatic change due to the anthropogenic inputs to the atmosphere of green-house gases and sources of acidity. Large rivers will clearly respond and change accordingly and therefore, changes to the Changjiang basin should be documented extensively. The aim of this paper is to decipher the different sources of solutes controlling the chemical composition of the dissolved load of the rivers draining the Changjiang basin and to investigate parameters controlling the chemical weathering at the Changjiang watershed scale.

In addition to CO_2 (atmospheric and mainly produced in soil), other sources of acidity contributes to the dissolution of rocks, hence, we will pay particular attention to other sources of protons involved in chemical weathering reactions, especially the role of sulphuric acid in the enhancement of the weathering rates. Several studies have shown the importance of sulphuric acid derived from the oxidation of pyrite at a regional scale, such as Han and Liu (2004), Xu and Liu (2007) for Southwestern China and at a larger scale, such as Galy and France-Lanord (1999) for the Ganges–Brahmaputra basin, Spence and Telmer (2005) for the Canadian Cordillera and Calmels et al. (2007) for the Mackenzie basin. In addition, sulphur emissions to the atmosphere and acidification of rain may also play a significant role in the increase of weathering rates. This reveals to be a major issue in China, despite efforts of the authorities to reduce the atmospheric emissions of SO_2. This work will allow us to ultimately estimate the CO_2 consumption by rock weathering for the Changjiang basin.

Another important issue we tackle in this study is the impact of human activities on the solute concentrations of the Changjiang basin rivers. Although the anthropogenic contribution to the chemical composition of the dissolved load of the Changjiang basin rivers has been demonstrated in previous studies (Chen et al., 2002; Qin et al., 2006), it was not previously assessed.

2. NATURAL SETTINGS OF THE CHANGJIANG DRAINAGE BASIN

2.1. Topography and geology

The Changjiang River, with a length of 6300 km, is the 3rd longest river in the world and the longest in China. Its drainage basin is situated between 25°N and 35°N and 90°E and 122°E, and covers a total area of 181×10^4 km^2, about 1/5 of China (Fig. 1). From its spring in the Qinghai–Tibet Plateau to the East China Sea, the Changjiang River has a fall of over 5400 m. Its upper, middle, and lower reaches are geographically divided by Yichang of Hubei Province (located right below the Three Gorges Dam) and the Poyang Lake of Jiangxi Province, and cover 100×10^4, 68×10^4 and 12×10^4 km^2, respectively. The section above Yibin in the Upper Reach where the Changjiang is called Jinshajiang, accounts for 95% of the Changjiang total fall (5100 m). The Changjiang basin can be divided into three physiographic provinces (Fig. 1). The first one, generally at 3500–5000 m in altitude, is composed of the southern part of the Qinghai province, the Sichuan Plateau and the mountainous valley regions of the Hengduan Mountains. The second one, generally at 500–2000 m in elevation, consists of the Qinba mountainous area, the Sichuan basin and the mountainous regions in Hubei and Guizhou. The third physiographic provinces, generally below 500 m in altitude, cover the Huaiyang mountainous area, the hilly area in the southern Changjiang, the Middle and Lower Reaches plains.

A simplified geological map is shown in Fig. 2. The Changjiang watershed is mainly overlain by sedimentary rocks composed of marine carbonates, evaporites and alluvium from Precambrian to Quaternary in age. Carbonate rocks are widely spread over the basin and are particularly abundant in the southern part (Yunnan, Guizhou and western Hunan Provinces) and the sub-basin of the Hanjiang (Chen et al., 2002). Coal strata are inter-bedded with carbonates especially in the southern basin and these coal deposits are rich in sulphides. Evaporites are mainly present in the Upper Reach of the Changjiang whereas rivers of the Poyang Lake sub-basin drain mainly metamorphic rocks.

2.2. Hydrology and land cover

Except for the source area characterized by high elevation and cold climate (mean temperature <4 °C), the Changjiang basin is submitted to a subtropical monsoon climate, temperate and humid (mean temperature 16–18 °C for the Middle and Lower Reaches). Annual rainfall amount averages 1100 mm and is unevenly distributed, decreasing gradually from southeast to northwest, from 1644 mm/year for the Lower Reach and 1396 mm/year for the Middle Reach to 435 mm/year for the Upper Reach (Chen et al., 2001). Surface runoff is the major water supply of the Changjiang watershed, accounting for 70–80% of the total water discharge (Chen et al., 2002).

Floods in the Changjiang basin are formed by storms which are concentrated between May and October. The rainy season occurs earlier in the Middle and Lower Reaches than in the Upper Reach, the earliest affecting the Dongting Lake and Poyang Lake systems between April and July. The period from May to August accounts between 50% and 65% of the annual total precipitation (Chen et al., 2001). The temporal and spatial distribution of rainfall in the wet season directly impacts sediment transport as the sediments discharge being concentrated during the rainy season. Before the completion of the Three Gorges Dam project, the suspended load averaged 434×10^6 tons/year at Yichang and 352×10^6 tons/year at Datong, the most downstream control station not marked

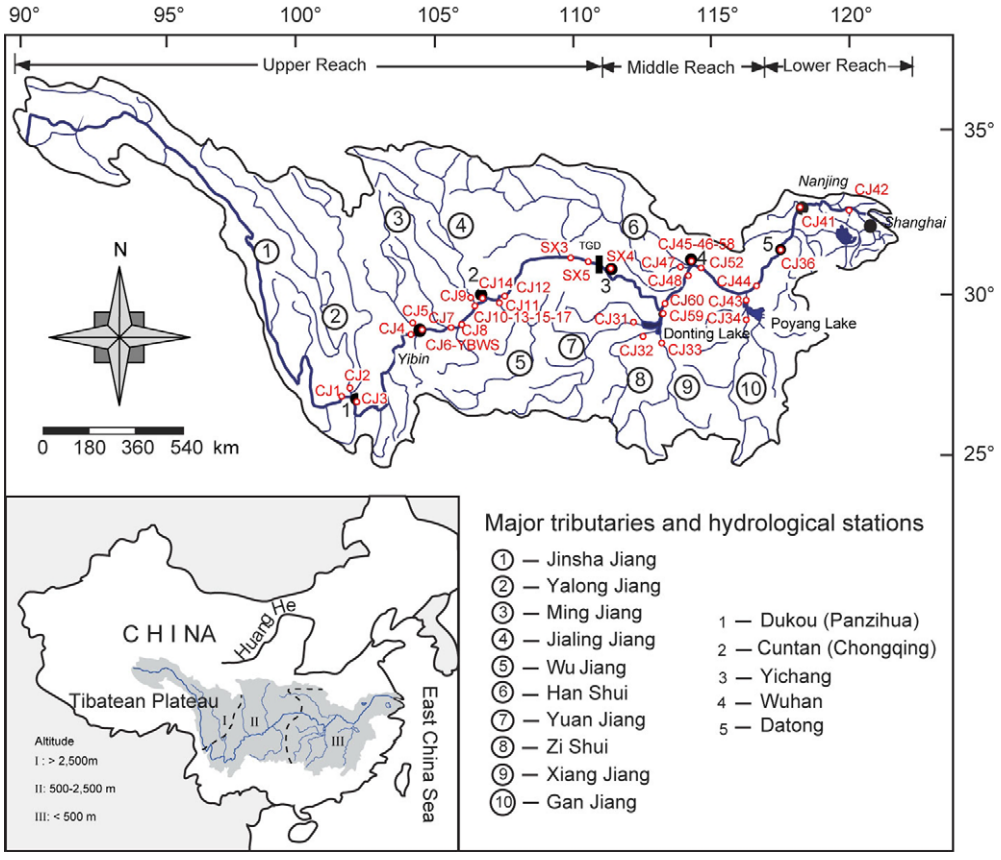

Fig. 1. Changjiang watershed and samples location.

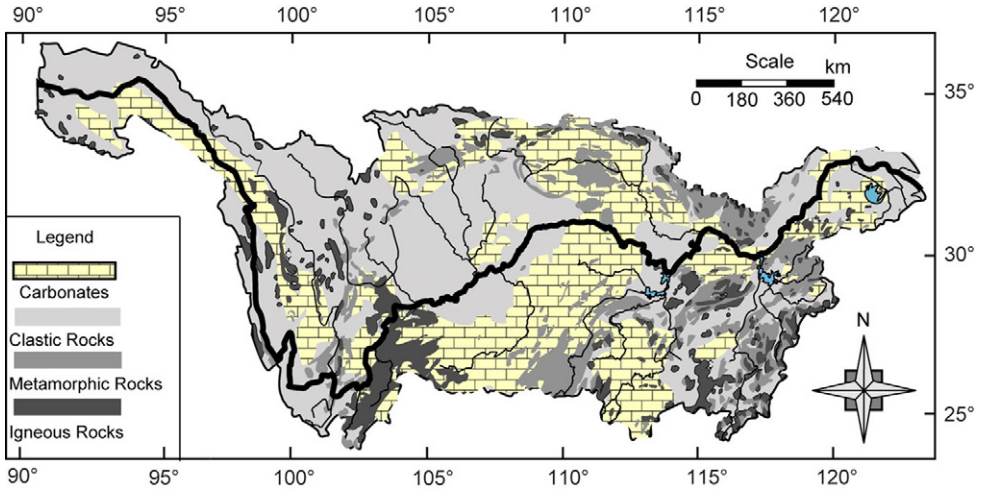

Fig. 2. Geological map of the Changjiang basin. Modified from Chen et al. (2002) and Li et al. (2007).

by tidal influence, during the period 1986–1998 (Yang et al., 2002).

The Changjiang basin contains 35% of the national population and the mean population density is around 226 h/km^2 (Liu et al., 2003). Population is unevenly distributed and mainly concentrated in the Sichuan basin, the Middle and Lower Reaches. Natural vegetation is mainly distributed in the mountainous and hilly areas whereas cultivated landscapes prevail on the plains. About 24% of the national arable land is located in the Changjiang basin and many industries are established in the basin. About 32% of the national gross output for agriculture and 34.5% of the national gross output for industry are produced in the basin (Xing and Zhu, 2002).

Cultivated land represents about 13% of the watershed mainly located in the Sichuan basin, the Middle and Lower Reaches (Xing and Zhu, 2002) and the forest area includes 30×10^4 km^2 covering 17% of the surface area. Due to the high level of development of the valley, pollution is a crucial issue for the Changjiang watershed (Fu et al., 2007) which collects the domestic/industrial waste water with or without treatment, slag and field waters.

3. SAMPLING AND ANALYTICAL METHODS

The Changjiang main channel and its largest tributaries (Yalongjiang, Minjiang, Jialingjiang, Wujiang, Poyang Lake, Hanshui and Dongting Lake) were sampled during August 2006 (Fig. 1). Samples were collected from the bank at a depth ranging from 50 cm to 1 m and from the middle of the river when a boat was available. The sampling was completed by the collection of samples of urban waste water in Yibin (YBWS) and from a small urban river in Wuhan (CJ58) (Fig. 1) contaminated by industrial and domestic effluents.

During sampling, 10–20 l of water were collected, stored temporally in acid-washed containers, and filtered few hours after collection through pre-washed 0.2 μm Sartorius® cellulose acetate filters. The first litre was discarded and the following ones were stored in acid-washed polyethylene bottles for analysis after acidification to pH 2 with double-distilled HCl. Two aliquots, one acidified for cations analysis and another non-acidified for the anions determination were prepared.

The suspended particulate matter (SPM) collected on the filters were removed in the clean laboratory using Millipore® MilliQ water and the solution containing the SPM were evaporated at 55 °C. The solid residue was then weighted and the SPM concentrations of the samples deduced.

The *T*, EC and pH were measured in the field and the alkalinity was determined with the Gran titration method a few hours later. Major cations (Ca, Na, K, and Mg), Si and Sr concentrations were measured by ICP-OES with a precision better than 5%. Anions (F, Cl, NO_3, and SO_4) concentrations were determined by ionic chromatography Dionex 120 with a precision of 5%. For all the samples, the inorganic charge balance is better than 10%.

The Sr isotopic compositions of the water samples were measured by MC-ICPMS on a Nu Plasma Instrument (Lang et al., 2006) after chromatographic separation on cationic exchange resin (Blum and Erel, 1997). Accuracy of the measurement was checked by running the NBS 987 standard ($n = 17$) which yielded a mean $^{87}Sr/^{86}Sr$ of 0.710248 ± 13 ($2\sigma_{error}$).

4. RESULTS

4.1. Major elements

The rivers of the Changjiang basin have total dissolved solids (TDS) ranging from 83 to 320 mg/l. The lowest values, 83 and 105 mg/l, are observed for the Poyang Lake and its main tributary, the Ganjiang River, respectively. TDS levels ranging from 140 to 168 mg/l were measured in the other freshwater lake, Dongting Lake, and its tributaries (Yuanjiang, Zi Shui and Xiangjiang) and are lower compared to the other Changjiang tributaries and main channel. The contribution of these two freshwater systems to TDS levels measured in the Changjiang main channel (Fig. 3) is obvious. The highest TDS value measured in the upper reach of the Changjiang may be related to the contribution of evaporite dissolution (high Na and Cl concentrations). In general, TDS values of the Changjiang main channel decrease from the upper to the lower reach with marked influence due to inputs from the two freshwater lakes, Poyang Lake and Dongting Lake. Major element concentrations in the collected water samples vary dramatically. For example, sodium concentrations range from 95 to 1390 μmol/l and a clear contrast is observed between the upper reach of the Changjiang basin printed by the dissolution of evaporites and the middle/lower reaches which

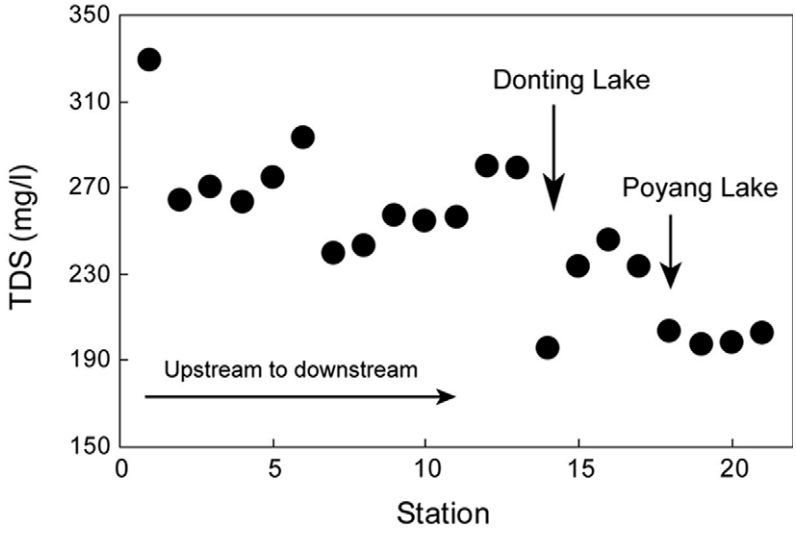

Fig. 3. Variation of the TDS of the Changjiang main channel from upstream to downstream.

are supplied by the fresh water lakes, Dongting Lake and Poyang Lake.

With an exception of the Jinshajiang at Panzhihua (CJ1), Ca is the major cation with concentrations ranging from 260 μmol/l (Poyang Lake) to 1080 μmol/l (Jialingjiang, CJ15). Magnesium concentrations range from 88 μmol/l (Poyang Lake) to 453 μmol/l (Jinshajiang at Panzhihua, CJ1). The Ca/Mg and Ca/Na ratios present also distinct values between the upper and the middle reaches, ranging from 2 to 5.5 and from 0.6 to 7.5, respectively. The highest values are observed for the Yuanjiang, Zi Shui, Xiangjiang and the Dongting Lake.

Carbonate species (CO_2dis, HCO_3, CO_3), calcite saturation index (CSI) and pCO_2 were calculated based on alkalinity, pH and T field data using the program of Zeebe and Wolf-Gladrow and the thermodynamic database provided with it available at http://www.awi-bremerhaven.de. All the samples except for that collected in the Poyang Lake (CJ43) are supersatured relative to calcite with CSI ranging from 0.2 to 2.4. Although supersaturation with respect to calcite does not imply the occurrence of calcite precipitation and that presence of inhibitors such as dissolved organic matter (Lebron and Suarez, 1996) prevents calcite precipitation, secondary calcite deposition can exert a significant control on riverine chemistry and calcium budget (Tipper et al., 2006). In the case of the Himalaya, it was established that up to 70% of the dissolved Ca was removed by precipitation (Jacobson et al., 2002; Bickle et al., 2005). The absence of any relationship in our data between the CSI and either the Sr/Ca molar ratios or the Mg/Ca molar ratios (Jacobson et al., 2002) does not preclude secondary calcite precipitation but we have no definitive arguments in favor (or against) the occurrence of such a process (Dalai et al., 2002; Wu et al., 2005).

HCO_3 is the most important anion (from 330 to 2380 μmol/l) and accounts for between 55% and 75% of the total anions. Cl and SO_4 are the second most important anions with concentrations ranging from 30 to 1134 μmol/l and from 92 to 588 μmol/l, respectively. A decrease of the Cl concentrations is obvious in the Changjiang main channel from upstream to downstream reflecting the contribution of evaporites in the upper reach and fall to around 250 μmol/l in the lower reach.

The NO_3 concentrations range from 4 to 95 μmol/l on the whole basin and increase from upstream (6 μmol/l, CJ1) to downstream (67 μmol/l, CJ42) along the Changjiang main channel. The lowest values are consistent with the concentrations measured in rainwater (Larssen et al., 1999; Aas et al., 2007) and the increase can be obviously related to the agriculture/urban releases into the aquatic system.

F concentrations are less variable, ranging from 5 to 15 μmol/l and are in the same range as those measured in precipitation (Larssen et al., 1999; Aas et al., 2007). According to Larssen et al. (1999), F in precipitation is mainly derived from coal combustion and the increase from upstream to downstream could be linked to the emissions from the industrialized area located in the center of the basin.

The Si concentrations range from 63 to 308 μmol/l. The highest concentrations are observed for the Ganjiang and the Poyang Lake, which drain silicate rocks (Fig. 2). For the Changjiang main channel, they present a narrow range from 139 to 202 μmol/l and increase from upstream to downstream.

4.2. Strontium isotopes

The Changjiang main channel sample (CJ36) collected at Datong which is representative of the entire basin and not influenced by tidal phenomenon, has a $^{87}Sr/^{86}Sr$ ratio of 0.7111, slightly higher than the previous values reported by Gaillardet et al. (1999b) and Wang et al. (2007b) around 0.7107. Overall, the Sr isotopic compositions are highly variable within the whole basin and range from 0.7083 for the Wujiang (CJ11) to 0.7153 for the Ganjiang (CJ34). The pattern of the Sr isotopes evolution of the Chanjiang main channel is given in Fig. 6. The Sr isotope ratios increase from 0.7103 to 0.7109 after its junction with the Yalongjiang (0.7121), then the ratio fluctuates between 0.7109 and 0.7111. When the Changjiang is joined by the Wujiang (0.7083), the $^{87}Sr/^{86}Sr$ ratio sharply decreases to 0.7105. The lower values for the Upper Reach are measured in the Three Gorges Dam and at Yichang with a $^{87}Sr/^{86}Sr$ value around 0.7103. The Middle Reach is marked by the contribution of the Dongting Lake (CJ59) ($^{87}Sr/^{86}Sr = 0.7119$) and the Poyang Lake (CJ43) ($^{87}Sr/^{86}Sr = 0.7151$).

4.3. Long-term evolution of the solute concentrations in the rivers of the Changjiang basin

In a previous study, Chen et al. (2002) have compiled the solute concentrations data of the Changjiang Basin rivers monitored at 191 stations for the period 1958–1990. The available data are average for the studied period of major elements especially for Cl, SO_4, Ca, Mg and Na + K. These authors observed a long-term evolution of the SO_4 and Cl concentrations they interpreted as a consequence of the increase of industrial and agricultural activities in the basin. They attributed the increase of SO_4 to atmospheric depositions and the Cl concentrations increase to the discharge of municipal and domestic sewages.

The Cl concentration measured at Datong, this last value is twofold the concentrations measured at the same approximate locations in previous studies (Gaillardet et al., 1999b; Chen et al., 2002). Such an increase of the Cl concentrations compared with the data of Chen et al. (2002) is obvious for other locations along the Changjiang main channel (Fig. 4), while the deviation between the values of the two studies seems to increase from upstream to downstream.

For SO_4, the same observation concerning the long-term increase of the concentration compared to the studies of Gaillardet et al. (1999b) and Chen et al. (2002) can be made and may confirm the conclusions of Chen et al. (2002) on the rise of the atmospheric depositions linked to coal burning but may also reflect the increase of the release of domestic/industrial effluents into the Changjiang watershed.

The sum Na + K follows the same trend as Cl and SO_4 (Fig. 4) whereas Ca and Mg concentrations remain roughly

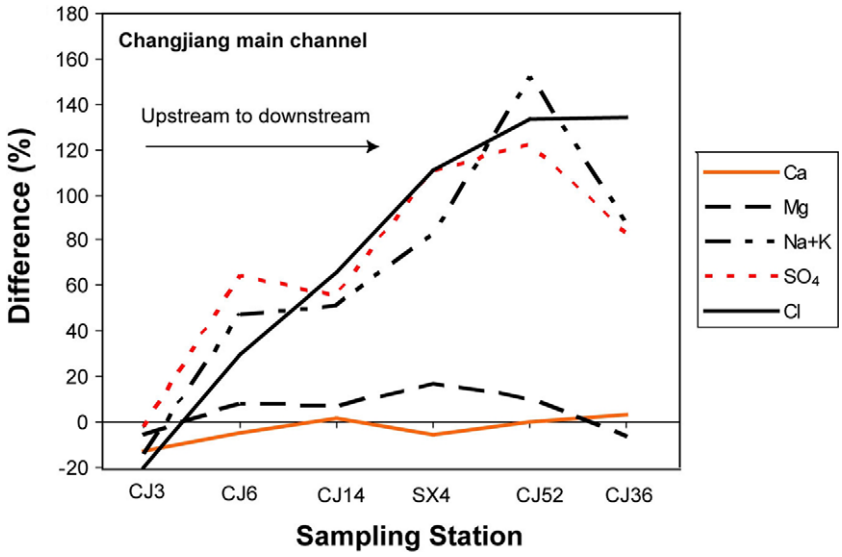

Fig. 4. Evolution of the relative difference between the major element concentrations measured in this study and the data reported in Chen et al. (2002) along the Changjiang main channel. The relative difference is expressed as $(X - X_0)/X_0$ where X denotes the concentration of an element X measured in this study and X_0 the concentration of the same element reported in Chen et al. (2002).

at the same level as those reported by Chen et al. (2002). The Ca concentration measured in this study is lower than the value of 973 μmol/l reported by Gaillardet et al. (1999b) at Nanjing (Fig. 1).

Regarding the main tributaries, all the samples follow the same long-term increase of SO_4 concentrations (Fig. 5). With the exception of few samples, Cl concentrations also display this trend. For example, in the case of the Ganjiang (CJ34), the Cl and SO_4 concentrations measured in the course of this study, 217 and 92 μmol/l, respectively, are 2- to 3-fold higher than those compiled by Chen et al. (2002) for the period 1958–1990. For the cations, the concentrations are generally higher than those reported in Chen et al. (2002).

5. DISCUSSION

In the following discussion, we attempt to quantify the contribution of the different sources of the solutes to the river by an inversion method (Negrel et al., 1993; Gaillardet et al., 1999b; Roy et al., 1999; Millot et al., 2003; Chetelat and Gaillardet, 2005; Wu et al., 2005; Moon et al., 2007). The model postulates that the chemical composition of the dissolved load of the rivers is the result of a mixing between different water masses bearing the chemical signature of different sources. Thus, one limitation of this approach is that secondary processes such as secondary phases precipitation that modify the signature of the source are not taken into account in the model (Gaillardet et al., 1999b; Wu et al., 2005; Moon et al., 2007). Especially, secondary calcite precipitation mentioned above and its consequences on the Ca budget and the drawdown of the CO_2 consumption rates by carbonate weathering can not be assessed. The first step of the model (Appendix A) is the identification of the sources of solutes and the characterization of their chemical signatures.

5.1. Sources of solute and characterization of the end-members

5.1.1. Atmospheric inputs

Estimation of the atmospheric inputs is the first step in deciphering the contribution of the different sources of solute in surface water at the watershed scale. Different approaches can be used to evaluate the atmospheric contribution to the chemical composition of river waters. The most commonly used element in these approaches is Cl. In pristine areas, concentration of Cl, provided that the contribution of evaporites is negligible, is assumed to be entirely derived from atmosphere and by using the Cl-normalized elemental ratios of rainwater, concentrations of other elements can be corrected with regard to the contribution of atmospheric deposition (Stallard and Edmond, 1981; Negrel et al., 1993). Unfortunately this approach is restricted to pristine areas and cannot be applied to riverine systems impacted by anthropogenic inputs due to the contribution of both agriculture and urban effluents to the river Cl budget (Roy et al., 1999). Han and Liu (2004) chose to correct the atmospheric contribution to the dissolved load of rivers located in the Wujiang basin based on the mean Cl concentration measured in a spring non affected by human activities. Xu and Liu (2007) recently adopted a similar method in studying water geochemistry of the Nanpanjiang and Beipanjiang rivers in the upper reach of the Xijiang basin and used the mean Cl concentration measured in rainwater (Han and Liu, 2006) collected in a site within the watershed. Although this approach is justified for small watersheds, in the case of the Changjiang basin, it is difficult to assume a constant Cl atmospheric input for the whole watershed. Larssen et al. (1999) report Cl concentrations in rainwater collected in different provinces drained by the Changjiang, which range from 15 to 30 μmol/l. Recently, Aas et al. (2007) have compiled the Cl concentrations

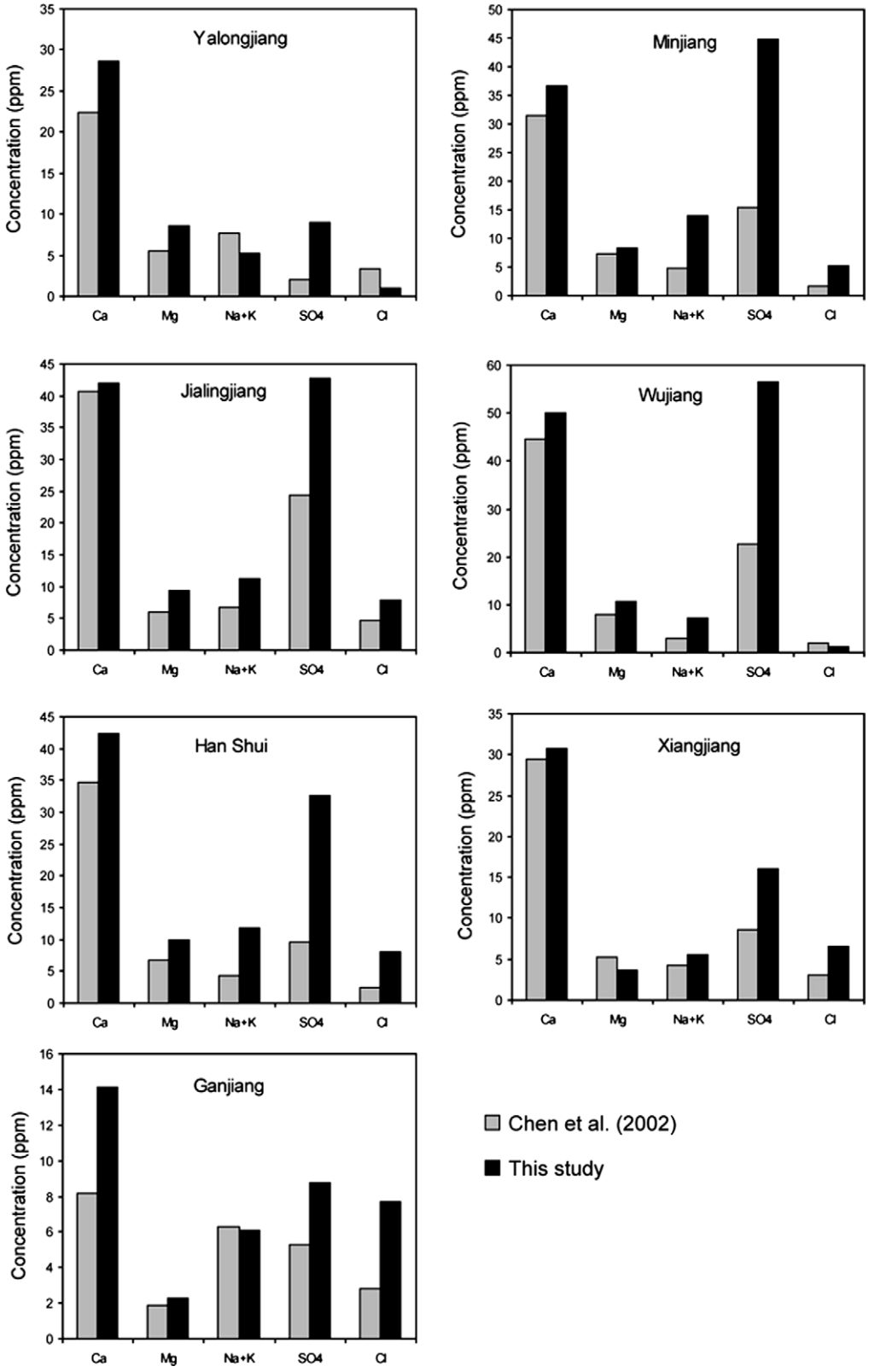

Fig. 5. Comparison of the chemical composition measured for water of some tributaries during this study with the data reported in Chen et al. (2002).

measured in bulk precipitations for non-urban area which range from 5 to 26 μmol/l. Higher mean Cl concentrations of 140 μmol/l were reported for the Nanjing area by Tu et al. (2005) and 50 μmol/l for the Taihu Lake basin by Luo et

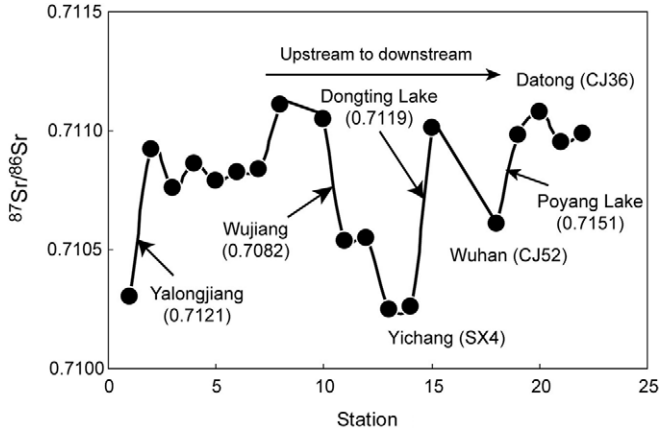

Fig. 6. Evolution of the Sr isotopic compositions measured in the Changjiang main channel from upstream to downstream. In brackets are the $^{87}Sr/^{86}Sr$ values of the selected tributaries.

al. (2007). For all of these studies, contribution of sea-salt dissolution is minor and the high Cl concentrations reflect the importance of the anthropogenic emissions to the atmosphere. In the following discussion, we will adopt the strategy used in the case of the Seine River by Roy et al. (1999) which takes into account the variability of the chemical composition of rainwater. The authors used the Cl concentrations as well as the Na-normalized ratios for the different elements measured in rainwater at different sites in the basin to correct from the atmospheric inputs. Instead of Cl, we will prefer to use the F concentrations as an indicator of the atmospheric contribution. As reported above, the F concentrations range from 5 to 15 μmol/l and increase from upstream to downstream but are in the range of concentrations (median, 11 μmol/l) measured by Larssen et al. (1999) for precipitations, and in the range of concentrations (median, 7.5 μmol/l) reported by Aas et al. (2007) for bulk precipitations collected in non-urban sites. Hence, we will assume that all the F measured in the river water samples has an atmospheric origin. By using the F/Na ratios and the Na-normalized values compiled by Larssen et al. (1999), Aas et al. (2007) and Tu et al. (2005) for the lower part of the Changjiang basin, we will correct the other elements from the atmospheric contribution.

To our knowledge, Han and Liu (2006) reported the only study of Sr concentrations and isotopic compositions for rainwater collected in the Changjiang basin. They gave a mean Sr/Na molar ratio of 0.03 and a mean Sr isotopic composition of 0.7082.

5.1.2. Anthropogenic inputs

TDS reflects both the different lithologies drained by the river (cf. the highest TDS observed in this study for the sample influenced by evaporite dissolution, CJ1) but also can be used as an index of the land use and the effects of human activities on the water quality (Gaillardet et al., 1999a,b). In the case of the Changjiang, the use of TDS as an index of pollution is probably not suitable because of the high water discharge and dilution effect but the impact of the land use is obvious for some elements. If we focus on the Changjiang mainstream, we can observe a sharp increase in the nitrate concentration after it enters the fertile Sichuan basin and this increase can mainly be related to the fertilizers used for the agriculture. The case of chlorine is also characteristic but less obvious due to the contribution of evaporites dissolution. Applying a dilution factor of 0.04 (Zhang et al., 2003) between the upper reach (Dukou) and the lower reach (Datong) (Fig. 1), we estimate the contribution of evaporites at Datong is around 45 μmol/l for Cl, much lower than those observed around 270 μmol/l. This calculation assumed there is no contribution of Cl from evaporites between the two sampling locations (this is true at a first approximation) however the discrepancy between the observed value and the calculated one is large enough to reflect the contribution of other sources of Cl as urban effluents and in a lesser extent to agricultural inputs. A group of rivers from the Poyang Lake and Donting Lake areas present Cl/Na ratios greater than 1, ranging from 1.1 to 1.5 and are obviously impacted by human activities, i.e. agriculture and atmospheric deposition.

Ca, Mg and HCO_3 are commonly considered to be insensitive to pollution (Flintrop et al., 1996; Roy et al., 1999). However, in the case of the Minjiang, Qin et al. (2006) noticed that along Cl and SO_4, Ca is also influenced by human activities, though it is not clear how this anthropogenic Ca is supplied to the river. To estimate the composition of the urban end-member we refer to the analysis of the waste water sample collected in Yibin (YBWS) and the sample collected in a small urban river flowing in Wuhan (CJ58) excepted for NO_3. The YBWS samples presents a high NO_3 concentration with a NO_3/Na molar ratio close to 0.6 much higher than that reported in other studies close to 0 (Roy et al., 1999). By comparison, the NO_3/Na ratio measured for CJ58 is around 0.04 and that calculated from Lang et al. (2006) is about 0.05. For the other elements, the chemical ratios for the YBWS and CJ58 samples are respectively 0.83 and 1.3 for Ca/Na, 0.37 and 0.66 for Cl/Na, 0.15 and 0.2 for K/Na, 0.19 and 0.34 for Mg/Na, 0.45 and 0.45 for SO_4/Na, 0.0011 and 0.0025 for Sr/Na. The two $^{87}Sr/^{86}Sr$ ratios measured in the waste water samples are fairly constant at around 0.7102 (Table 1). The ratios used in our computation are summarized in Table 2.

Table 1
Chemical composition and Sr isotopic composition of rivers of the Changjiang basin

Sample	River, location	Latitude	Longitude	h *m*	pH	*T* (°C)	K (μM)	Na (μM)	Ca (μM)	Mg (μM)	Alk (mM)	DIC (mM)	F (μM)	Cl (μM)	NO_3 (μM)	SO_4 (μM)	H_4SiO_4 (μM)	TDS (mg/l)	Sr (μM)	$^{87}Sr/^{86}Sr$
CJ-1	Jinshajiang, Panzhihua	26°34.503′	101°37.551′	1001	8.00	22.6	52	1393	892	454	2.6	2.5	5.7	1135	6.2	352	144	321	3.2	0.710335
CJ-2	Yalongjiang, Panzhihua	26°40.127′	101°49.200′	1010	7.3	23.3	32	168	715	353	2.2	2.2	5.3	30	5.3	94	170	205	2.2	0.712092
CJ-3	Jinshajiang, Panzhihua	26°34.549′	101°51.109′	1000	7.95	25.4	42	783	805	404	2.3	2.3	6.9	557	4.0	221	152	256	2.4	0.710929
CJ-4	Jinshajiang, Yibin	28°42.164′	104°33.385′	293	7.85	26.4	44	622	850	418	2.5	2.3	6.7	440	24	276	159	262	2.5	0.710749
CJ-5	Minjiang, Yibin	28°48.779′	104°33.721′	266	7.8	31.5	66	496	916	343	1.9	1.9	7.7	146	88	467	123	243	2.4	0.710878
CJ-6	Jinshajiang, Yibin	28°46.074′	104°40.316′	261	8.02	27.5	55	598	888	376	2.2	2.1	7.3	307	52	381	145	255	2.5	0.710851
CJ-7	Jinshajiang, Luzhou	28°52.180′	105°25.921′	258	7.84	27.4	59	720	889	387	2.2	2.2	7.4	348	50	418	154	266	2.5	0.710779
CJ-8	Jinshajiang, Luzhou	28°54.801′	105°27.897′	235	7.8	28.1	64	703	980	404	2.3	2.3	11	377	76	465	174	285	2.6	0.710828
CJ-9	Jialingjiang, Chongqing	29°33.902′	106°28.632′	202	8.09	30.9	62	387	1048	390	2.2	2.2	8.5	223	64	445	129	261	3.5	0.710807
CJ-10	Changjiang, Chongqing	29°23.614′	106°31.474′	170	8.1	27.4	51	526	878	393	1.9	1.9	7.2	299	43	337	139	231	2.5	0.710867
CJ-11	Wujiang, Fuling	29°41.867′	107°24.485′	207	8.61	27.3	50	222	1247	444	2.3	2.0	9.4	158	95	588	138	273	3.7	0.708233
CJ-12	Changjiang, Fuling	29°46.270′	107°25.265′	136	8.15	27.3	52	533	951	418	2.1	2.0	9.0	329	54	355	141	248	2.7	0.710542
CJ-13	Changjiang, Chongqing	29°36.927′	106°45.238′	154	8.03	27	58	640	942	397	2.0	1.9	7.6	325	52	403	151	249	2.7	0.711055
CJ-14	Changjiang, Chongqing				7.87	26.8	57	554	949	379	1.9	1.9	7.8	332	72	387	153	246	2.6	0.710736
CJ-15	Jialingjiang, Chongqing	29°34.138′	106°33.463′	186	8.35	31.4	59	406	1083	403	2.5	2.3	9.6	238	65	462	63	269	3.4	0.711127
CJ-16	Changjiang, Wanzhou	30°47.421′	108°23.708′	166	8.15	28.8	55	601	962	417	2.1	2.0	8.4	378	42	334	nd	—	2.6	nd
CJ-17	Changjiang, Chongqing	29°32.979′	106°34.173′	170	8.00	29	58	528	957	366	1.7	1.7	7.9	315	83	396	154	234	2.6	0.711112
SX3	Three Gorges Dam Reservoir			95	nd	nd	53	607	942	381	2.2	—	9.2	423	57	363	143	—	2.8	0.710233

SX5	Three Gorges Dam Reservoir				8.17	28.7	57	602	970	407	2.5	2.3	11	380	51	356	144	271	2.9	0.710533
SX4	Changjiang, Yichang			75	7.8	28.7	55	619	956	385	2.3	2.3	9.5	425	63	365	136	270	2.8	0.710259
CJ-31	Yuan Jiang, Taoyuan	28°54.333′	111°29.146′	40	8.74	32	33	94	637	251	1.2	1.0	6.2	89	42	179	180	139	1.2	0.711886
CJ-32	Zi Shui, Yiyang	28°35.896′	112°21.767′	47	8.7	31	41	100	750	137	1.3	1.1	6.2	116	56	155	157	142	1.1	0.711560
CJ-33	Xiang Jiang, Changsha	28°07.364′	112°56.795′	70	7.28	31	60	140	765	146	1.3	1.4	8.8	183	80	166	186	168	1.0	0.712778
CJ-34	Gan Jiang, NanChang	28°40.206′	115°52.053′	79	7.3	30	69	147	351	96	0.5	0.5	13	217	56	92	308	105	0.7	0.715335
CJ-36	Changjiang, Datong	30°46.085′	117°38.324′	21	8.00	30.2	60	308	774	241	1.5	1.5	11	277	65	227	202	190	2.3	0.711150
CJ-41	Changjiang, Nanjing				8.15	30.5	60	318	797	248	1.5	1.4	11	287	64	241	194	191	2.4	0.710959
CJ-42	Changjiang, Zhangjiangang	31°58.785′	120°40.696′	12	8.25	30.6	61	421	747	269	1.6	1.5	11	302	67	245	192	195	2.5	0.711000
CJ-43	Poyang Lake	29°38.658′	116°12.224′	24	8.2	29.1	66	143	263	88	0.4	0.3	11	182	39	104	256	83	0.6	0.715138
CJ-44	Changjiang, Pengze	29°54.165′	116°32.493′	22	7.95	30.6	60	366	740	264	1.6	1.5	1	258	67	243	190	196	2.4	0.710989
CJ-45	Changjiang, Wuhan	30°37.180′	114°19.233′	27	8.15	30.8	58	410	939	352	2.1	2.0	11	257	59	304	152	237	2.8	nd
CJ-46	Han Shui, Wuhan	30°34.004′	114°15.180′	28	7.94	30.5	58	415	1057	410	2.5	2.5	15	229	45	341	133	272	2.7	0.711530
CJ-47	Han Shui, Wuhan	30°35.802′	114°04.845′	28	8.25	30.6	56	410	1050	407	2.5	2.4	13	216	41	322	121	261	2.7	0.711507
CJ-48	Changjiang, Wuhan	30°27.397′	114°11.814′	28	7.96	29.7	56	397	854	306	1.9	1.9	9.2	272	74	282	169	226	2.9	nd
CJ-52	Changjiang, Wuhan	30°40.747′	114°29.876′	24	8.1	29.4	56	409	864	305	1.9	1.9	9.8	283	75	285	166	225	2.5	0.710638
CJ-59	Dongting Lake	29°22.625′	113°04.721′		7.85	30.3	51	166	761	186	1.4	1.3	9.4	182	60	183	161	166	1.3	0.711892
CJ-60	Changjiang, Yueyang	29°38.079′	113°18.739′		8.16	30	55	351	762	243	1.6	1.5	8.8	266	60	217	162	188	2.0	0.711007
CJ-58	Waste water, Wuhan				nd	nd	179	909	1180	312	nd	—	19	604	43	406.6	nd	—	2.3	0.710180
YBWS	Waste water, Yibin	28°48.320′	104°34.848′	258	7.91	31.2	448	3016	2493	575	nd	—	18	1125	1478	1344.2	nd	—	3.5	0.710160

nd, not determined.
TDS = Na + K + Mg + Ca + Cl + SO_4 + NO_3 + HCO_3 + H_4SiO_4.

Table 2
Composition of the different end-members used in our calculation

	F/Na	K/Na	Mg/Na	Ca/Na	Cl/Na	N03/Na	Sr/Na	$^{87}Sr/^{86}Sr$
Atmosphere	0.7 ± 0.2	0.5 ± 2	0.6 ± 0.25	5 ± 3	2.8 ± 1.1	0.5 ± 4	0.03 ± 2	0.708–0.709
Urban	0	0.16 ± 7	0.2 ± 0.1	0.8 ± 2	0.6 ± 15	0	0.0021 ± 6	0.7101–0.7102
Agriculture	0	1.4 ± 0.4	0	0	5 ± 1	4 ± 1	0	—
Evaporites	0	0	0.01-0.5	0.15-5	1	0	0.0005-00.005	0.708–0.709
Carbonates	0	0	19 ± 9	50 ± 20	0	0	0.09 ± 3	0.708–0.709
Silicates	0	0.17 ± 7	0.2 ± 0.05	0.35 ± 15	0	0	0.003 ± 1	0.72–0.73

See text for details.

For the chemical signature of the agriculture end-member, we refer to the estimation of Roy et al. (1999), Zeng and Sun (1999) and Liu et al. (2006), and we assume that only Na, Cl and K are affected by agricultural inputs. Roy et al. (1999) estimated a Cl/Na and NO_3/Na molar ratios of 5 and 10, respectively, while Liu et al. (2006) reported NO_3/Cl molar ratios $\geqslant 1$ for waters impacted by farming pratices. For K, we use the estimations of Zeng and Sun (1999) who reported NO_3/K molar ratios for chemical fertilizers between 3 and 4. In our case, we used our algorithm (see Appendix A) to refine the agricultural end-member and obtained the best results for Cl/Na, NO_3/Na and K/Na molar ratios of 5, 4 and 1.4, respectively (Table 2), which are close to the values reported in these previous studies.

5.1.3. Weathering component

5.1.3.1. Evaporites dissolution. Although the contribution of evaporites is obvious in the upper Changjiang and its main tributaries (Yalongjiang, Minjiang and Jialingjiang) before the Three Gorges Dam, its estimation is not an easy task except for the CJ1 sample for which Cl and Na are well balanced. For the other samples, contributions of anthropogenic inputs and sulfides oxidation make the task harder. Furthermore, the source of evaporites is not unique and globally varies from a halite end-member to a gypsum end-member characterized by different SO_4/Na ratios. To estimate the chemical ratio of this evaporites end-member, we referred to the data measured in the rivers of the Changjiang basin compiled by Chen et al. (2002). Unfortunately, Na concentrations are not available, only the sum of Na and K, so we will consider the Cl concentrations (the Cl/Na in the evaporites is assumed to be 1). For the Minjiang, these authors reported SO_4/Cl ratios ranging from 0.2 to 4.5 (mean 2.2) with a value of 3.6 at the Gaochang hydrological station (Yibin). Contribution of pyrite oxidation to the SO_4 budget is mentioned in the basin in particular at the Duoyinping station (Qin et al., 2006). For this site, Chen et al. (2002) report a SO_4/Cl ratio of 3.6, thus the SO_4/Cl for the evaporites end-member should be lower.

For the Jialingjiang, no specific studies have been carried out and Chen et al. (2002) gave a range of SO_4/Cl ratio from 0.6 to 17 with a mean value of 3.4. The rivers draining the Wujiang catchment present higher SO_4/Cl ratios with a mean value around 5, (Chen et al., 2002), but as highlighted by Han and Liu (2004) and Jiang et al. (2006), a large proportion of the sulphate present in the rivers comes from the oxidation of sulfides. For the Han Shui and Xiangjiang, the SO_4/Cl molar ratios range from 0.5 to 2.5 and from 0.6 to 1.5, respectively. In the case of the upper Changjiang and the Yalongjiang, we will assume a SO_4/Na close to 0.17, as halite end-member (Millot et al., 2003). Assuming that Ca in evaporites is balanced by SO_4, in the following discussion, the Ca/Na molar ratio for the evaporites end-member ranges from 0.15 to 5. For Mg, we assume a Mg/Ca molar ratio of 0.1 in evaporites (Gaillardet et al., 1999b; Millot et al., 2003 and Wu et al., 2005) and that the K riverine budget is not affected by the evaporites dissolution.

5.1.3.2. Silicate weathering. To estimate the composition of the silicate end-member, we refer to previous studies (Gaillardet et al., 1999b; Millot et al., 2003; Han and Liu, 2004 and Wu et al., 2005). In the following discussion, Mg/Na, Ca/Na and Sr/Na are assumed to be close to 0.2, 0.35 and 0.003, respectively. Roy et al. (1996) and Wang et al. (2007b) reported Sr isotopes ratio between 0.718 and 0.725 for the insoluble phase of the Changjiang close to the values estimated for the Tibetan Sedimentary Series (Oliver et al., 2003) and those measured as well as in loess samples (Liu et al., 1994) and the silicate residues of loess samples collected in the Chinese Loess Plateau by Wang et al. (2007a). For the Sr isotopic composition of the silicate end-member, we assume a range of the $^{87}Sr/^{86}Sr$ from 0.72 to 0.73.

For the K/Na ratio, we assume a value of 0.17 close to that deduced by Millot et al. (2003) and observed in rivers draining silicates (Meybeck, 1986).

5.1.3.3. Carbonate weathering. As revealed by the high concentrations of both dissolved Ca and Mg, the solute composition is dominated by the dissolution of carbonates. Coupled with Sr data, major elements allow us to distinguish two types of carbonates, limestone and dolomite characterized by distinct Mg/Ca and Sr/Ca ratios. The samples collected in the Yuanjiang (CJ31), Zi Shui (CJ32), Xiangjiang (CJ33) fall close to the limestone end-member (Gaillardet et al., 1999b) and are characterized by Mg/Ca, Na/Ca and Sr/Ca ratios around 0.1, 0.02 and 0.0007, respectively.

In our calculation, we use a Sr isotopic composition for carbonates ranging from 0.708 to 0.709 and a Sr/Na ratio ranging from 0.006 to 0.012.

5.1.3.4. Sulphide oxidation. Based on major elements, estimation of the fraction of SO_4 coming from the oxidation of pyrite is difficult to assess and can overestimate or

underestimate the weathering fluxes coming from sulphuric acid dissolution. The most striking example of sulphide oxidation contribution is obtained for the Wujiang for which the contribution of evaporites is minor (Han and Liu, 2004). After correction of atmospheric and anthropogenic inputs, the remaining SO_4 is about 425 μmol/l, thus pyrite oxidation should represent 70% of the S budget for this river. The same estimation is given in Jiang et al. (2006) based on S isotopes, the $\delta^{34}S$ ranging from −7‰ to −4‰ for the Wujiang main stream in summer.

5.2. Chemical mass balance for the rivers of the Changjiang basin

For each elements and isotopic ratios, we can write mass balance equations with the assumptions discussed above.

$$[F]_{river} = [F]_{atmosphere}$$

$$[NO_3]_{river} = [NO_3]_{atmosphere} + [NO_3]_{agriculture}$$

$$[NO_3]_{river} = [NO_3]_{atmosphere} + [NO_3]_{agriculture}$$

$$[Cl]_{river} = [Cl]_{atmosphere} + [Cl]_{agriculture} + [Cl]_{evaporites} + [Cl]_{urban}$$

$$[K]_{river} = [K]_{atmosphere} + [K]_{agriculture} + [K]_{silicates} + [K]_{urban}$$

$$[Na]_{river} = [Na]_{atmosphere} + [Na]_{silicates} + [Na]_{evaporites} + [Na]_{urban} + [Na]_{carbonates} + [Na]_{agriculture}$$

$$\text{with} \quad [Cl]_{evaporites} = [Na]_{evaporites}$$

$$[Ca]_{river} = [Ca]_{atmosphere} + [Ca]_{silicates} + [Ca]_{evaporites} + [Ca]_{urban} + [Ca]_{carbonates}$$

$$[Mg]_{river} = [Mg]_{atmosphere} + [Mg]_{silicates} + [Mg]_{evaporites} + [Mg]_{urban} + [Mg]_{carbonates}$$

$$[Sr]_{river} = [Sr]_{atmosphere} + [Sr]_{silicates} + [Sr]_{evaporites} + [Sr]_{urban} + [Sr]_{carbonates}$$

$$(^{87}Sr/^{86}Sr)_{river} = \sum \alpha_i (^{87}Sr/^{86}Sr)_i$$

with α the proportion of Sr derived from the different sources and i stands for atmosphere, silicate, evaporites, urban and carbonate.

Instead of this set of equations, we used mass balance equations normalized to Na (see Appendices A, B, C for details). Note that this set of equations does not include a mass budget for the inorganic carbon system (HCO_3) in order to investigate the role H_2SO_4 in chemical weathering by checking the balance between HCO_3 ions (measured) and cations derived from carbonate and silicate weathering (calculated).

Although a few studies (Dalai et al., 2002; Singh et al., 2005) used the observed relationship between Si and Na corrected form the contribution from evaporites dissolution ($Na_{corrected} = Na_{river} - Cl_{river}$) to estimate the proportion of Na derived from silicate weathering, other authors stressed the importance of a biological control on the Si exportation fluxes (Huh et al., 1998; Viers et al., 2000; Ding et al., 2004; Gerard et al., 2008). As also reported in Huh et al. (1998) and Moon et al. (2007) for example, we do not observe such a relationship between Si and either Na or Na corrected from evaporites contribution according to the method used in these studies. One possible reason is that a part of Na is supplied by anthropogenic sources. Furthermore, in the case of Si, we might suspect a control by biological processes as it was highlighted for the Changjiang by Ding et al. (2004) based on Si isotopic compositions.

5.3. Results of the calculation

The calculated contributions of different weathering sources to the cationic TDS (mg/l) for the Changjiang main channel and its main tributaries are illustraded Fig. 7 and the values reported in Appendix B. Overall, at rare exceptions, rivers of the Changjiang basin are dominated by carbonate weathering, the contributions of which to the cationic dissolved load range from 40% to 80%. The lowest contributions are calculated for the upper Changjiang main channel (CJ1) dominated by evaporites weathering and the Ganjiang (CJ34) dominated by silicate weathering and anthropogenic inputs. The highest contributions are observed for the Yalongjiang (CJ2), Wujiang (CJ11) and the Xiangjiang (CJ33). For the Datong station, carbonates contribution is around 60%.

Contribution of silicate weathering is more variable, ranging from 5% for the Wujiang and the Xiangjiang to 19.5% for the Minjiang. For the Changjiang main Channel, the silicate contribution decreases upstream from downstream and reaches 10% at the Datong station. Contribution of evaporites to the cationic load ranges from 0% to 45% and accounts for less than 10% for the middle and lower reaches of the Changjiang. At the Datong station, we estimate a dissolved flux of 7×10^6 ton/year similar to the value reported by Gaillardet et al. (1999b).

Atmospheric inputs are in general minor, for the cations, their contribution ranges from 2% to 10% (for most of the samples around 5%) excepted for the Ganjiang (CJ34) for which the atmospheric inputs represent 13% of the total cations.

Contribution of human activities (communal/industrial inputs and agriculture) to the cationic TDS in the Changjiang main channel is variable, ranging from 0% for the headwaters of the basin to 20–30% at Chongqing (CJ14) and for the Three Gorges Dam Reservoir (SX5 and SX4). The evolution pattern of the human activities contribution to the cationic TDS for the Changjiang main channel is illustrated in Fig. 8. The general trend is an increase of anthropogenic contribution from upstream to downstream with a maximum at Chongqing. For the lower reach, the contribution approaches 15–20% and illustrates the great sensitivity of the Changjiang to the changes of land use in spite of the high water discharge of this river. The cationic TDS measured for the waste water samples collected at Yibin (YBWS) and Wuhan (CJ58) are 201 mg/l and 83 mg/l respectively. Using the Changjiang water discharge and the cationic TDS derived from anthropogenic activities calculated at Datong (27,400 m^3/s and 7 ± 3 mg/l, respectively), we estimate a flux of waste water of $31 \pm 12 \times 10^9$ m^3/year or $75 \pm 30 \times 10^9$ m^3/year calculated with either the cationic TDS measured for the YBWS sample

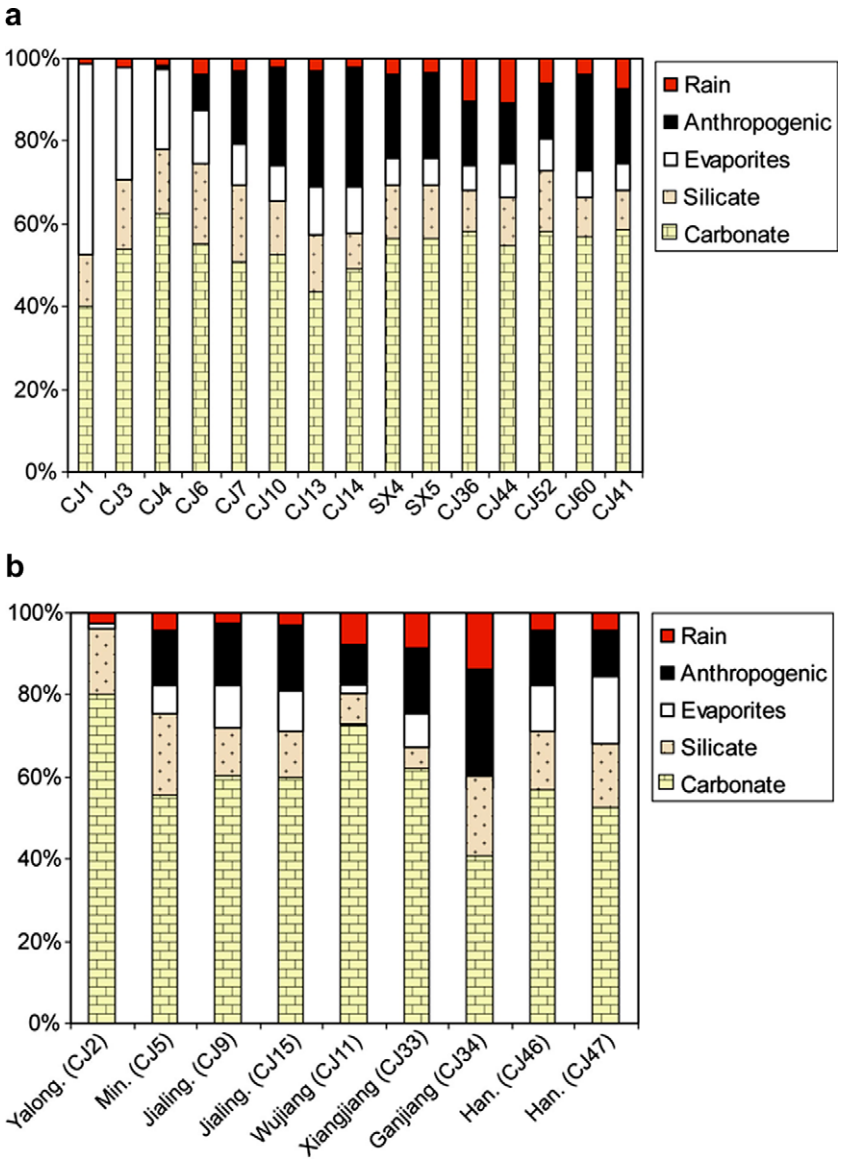

Fig. 7. Calculated contributions of the different reservoirs to the cationic TDS (mg/l) with the inversion method for the Changjiang main stream (a) and some major tributaries (b). The anthropogenic contribution includes the agricultural and the domestic/industrial waste water inputs.

or that measured for the sample CJ58, respectively. These estimations are in the same range of magnitude than the value of $30 \times 10^9\ m^3$ reported in Huang et al. (http://www.mwr.gov.cn/english1/20060110/20060110103906WSXRED.pdf) for the year 2000. Strictly speaking the sample CJ58 is not a waste water sample but a sample obtained from a small river flowing through an urban environment (cf. Sampling and analytical methods section), thus dilution by rainwater may explain the lower cationic TDS value compared to that of the YBWS sample and hence the higher flux of waste water. Nevertheless, considering the uncertainties, this last value is reasonable and also in agreement with the flux of waste water into the Changjiang reported for the year 2000.

On a long term scale, the Changjiang has experienced an increase of the contribution from human activities. As illustrated in Fig. 4 we observed a sharp increase of the concentrations for Cl, SO_4 and Na + K when compared with the data of Chen et al. (2002) whereas the concentrations of Ca and Mg remain fairly constant between the two studies.The difference between the two groups of elements can be interpreted by the greater sensitivity of Cl, SO_4 and Na + K to human disturbances than Ca and Mg, which are dominated and buffered by carbonate weathering.

5.4. Chemical weathering in the Changjiang basin

As weathering index, we use the rate of cationic weathering rates (Millot et al., 2003) expressed in ton/km^2/year which are calculated by the following equations:

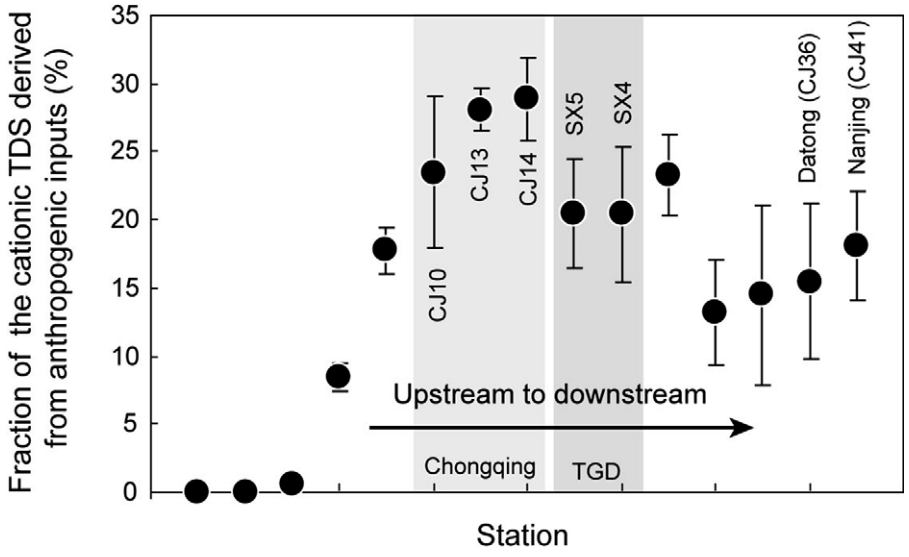

Fig. 8. Evolution of the contribution of anthropogenic inputs to the cationic TDS measured in the Changjiang main channel from upstream to downstream.

$$\Phi_{sil} = \Phi Na_{sil} + \Phi K_{sil} + \Phi Ca_{sil} + \Phi Mg_{sil}$$
$$\Phi_{carb} = \Phi Ca_{carb} + \Phi Mg_{carb}$$

The rates are calculated with the mean monthly water discharges for August 2006 (Tables 3 and 4) available at http://sqqx.hydroinfo.gov.cn/websq/sqrb (in Chinese) and averaged over 1 year. With the exception of the Jialingjiang, Wujiang and Yuanjiang for which the water discharge (expressed in m^3/s) measured in August represents only 65% of the mean value (expressed in m^3/s) for the year 2006, for all the samples, it represents between 100% to 130% of the mean annual value. In the case of the Minjiang, Qin et al. (2006) have shown that the TDS fluxes calculated using the annual average value of a monthly sampling and a single water analysis during the beginning or the fall of the peak discharge gave similar results within 20–30%.

The cation–silicate weathering rate is highly variable from one sub-basin to another and varies by more than one order of magnitude, ranging from 0.7 ton/km^2/year for the Wujiang to 7.1 ton/km^2/year for the Minjiang For the Changjiang main channel, the rate calculated at different sampling sites slightly increases from upstream (1.7 ton/km^2/year at Chongqing) to downstream (3.3 and 2.4 ton/km^2/year at Wuhan and Datong, respectively). This increase of the silicate weathering rate from upstream to downstream is in agreement with the conclusion of Xue et al. (2005), who studied the statistical distributions of major chemical compositions (HCO_3 and Ca) and TDS for the rivers of the Changjiang basin. The authors concluded runoff and silicate weathering (as well as anthropogenic inputs) explained variability in chemical composition between rivers draining the Upper and Lower reaches with those draining the Lower reach.

At a first approximation, we will consider that the fluxes calculated for the main channel at Chongqing (CJ14) are representative of the weathering fluxes for the Tibetan Plateau. Thus, this value is similar to the silicate cation flux of 1.3 ton/km^2/year reported for the Tibetan Plateau by Singh et al. (2005). The flux of cations derived from silicate weathering estimated at Datong, 4.1×10^6 ton/year is higher the value calculated by Gaillardet et al. (1999b), 2.5×10^6 ton/year as well as the flux of Ca + Mg derived from silicate weathering, 43×10^9 mol/year and 29×10^9 mol/year, respectively. Nevertheless, these fluxes remain comparable considering the uncertainties affecting the estimations (Table 4). Furthermore, these higher values could be used to explain the more radiogenic Sr isotopic composition observed at Datong compared with the value reported by Gaillardet et al., 1999b. The cationic carbonate weathering rate is also variable, ranging from 6 ton/km^2/year for the Jialingjiang to 21 ton/km^2/year for the Xiangjiang and reaches 14 ton/km^2/year for the Changjiang at Datong. The carbonate TDS calculated in this study for the Datong station, 62×10^6 ton/year, is much lower than the value reported in Gaillardet et al. (1999b), 101×10^6 ton/year. Assuming that all the Ca and Mg come from the dissolution of carbonates, the flux reaches 80×10^6 ton/year but is still lower than the estimation of these authors. For the Wujiang, Han and Liu (2004), report a carbonates weathering rate of 97 ton/km^2/year also higher than that calculated in this study, about 30 ton/km^2/year. Note that this rate was calculated for only a portion of the Wujiang catchment, about 75% of the total surface area. The discrepancy can be mainly explained by the lower water discharge measured during the course of this study and the surface area of the drainage basin, using the same water discharge of 327×10^8 m^3/year and surface area of 6.7×10^4 km^2, the carbonates weathering rate reaches 70 ton/km^2/year closer to the estimation of Han and Liu (2004).

Globally, the speed of chemical erosion calculated by using a mean density of 2.7 and 2 for silicate and carbonate rocks, respectively, range from 10 mm/kyr for the

Table 3
Chemical weathering rates and CO_2 consumption for the Changjiang main tributaries

Sample	River, location	Surface area (10^4 km^2)	Water discharge (m^3/s)	SPM (mg/l)	Silicates				Carbonates			Evaporites	Total rock weathering
					Φsil (ton/km^2/year)	Cat sil[a] (10^6 ton/year)	Ca + Mg sil (10^9 mol/year)	CO_2 cons. (10^9 mol/year)	Φcarb (ton/km^2/year)	$TDS_{carb.}$[b] (10^6 ton/year)	CO_2 cons. (10^9 mol/year)	$TDS_{evap.}$[c] (10^6 ton/year)	TDS[d] (10^6 ton/year)
CJ-5	Minjiang, Yibin	13.3	2,596	354	7.1 ± 0.3	0.94 ± 0.04	11 ± 1	12–45	20 ± 1	7.2 ± 0.2	35–75	1.1 ± 0.3	9.3 ± 0.5
CJ-9	Jialingjiang,Chongqing	15.8	818	6	1.2	0.2	1.8 ± 0.1	8.6 ± 0.4	6.2	2.6 ± 0.2	28 ± 1	0.6	3.4 ± 0.1
CJ-15	Jialingjiang, Chongqing	15.8	818	6	1.2	0.2	1.9 ± 0.1	8.3 ± 0.4	6.3	2.7 ± 0.2	28 ± 1	0.6	3.5 ± 0.2
Mean	Jialingjiang, Chongqing				1.2	0.2	1.8	8.5	6.2	2.6	28	0.6	3.4
CJ-11	Wujiang, Fuling	8.79	534	10	0.69 ± 0.05	0.06	0.8 ± 0.1	0–2.9	10 ± 0.4	2.3	7.6–8.9	0.07 ± 0.02	2.4 ± 0.1
CJ-33	Xiang Jiang, Changsha	9.47	2,591	21	1.7 ± 0.3	0.16 ± 0.01	1.9 ± 0.6	7.5 ± 1.6	21 ± 9	5.3 ± 0.9	54 ± 24	0.9 ± 0.3	6.3 ± 1.2
CJ-34	Gan Jiang, NanChang	8.09	2,236	10	3.2 ± 0.5	0.26 ± 0.03	3.6 ± 0.9	12 ± 2	9 ± 3	1.8 ± 0.2	19 ± 6	0	2.1 ± 0.3
CJ-46	Han Shui, Wuhan	15.9	1,306	43	2.4 ± 0.3	0.38 ± 0.04	4.3 ± 0.8	18 ± 2	9 ± 1	3.7 ± 0.2	43 ± 5	0.9 ± 0.4	5.4 ± 0.6
CJ-47	Han Shui, Wuhan	15.9	1,306	59	2.5 ± 0.4	0.40 ± 0.05	4.6 ± 1.4	19 ± 3	9 ± 1	4.1 ± 0.2	40 ± 5	1.4 ± 0.4	5.6 ± 0.6
Mean	Han Shui, Wuhan				2.45	0.39	2.5	19	9	3.9	41.5	1.2	5.5

The CO_2 consumption rates are based on the cationic contribution derived from the inverse model (see Appendix C). The incertitudes are estimated from the inverse model.

[a] The flux of cations derived from silicate weathering is related to the cationic weathering rate by Cat sil = Φsil × S where S stands for the surface area of the basin.

[b] TDS values are calculated based on the sum of the cations estimated from the inverse model and their stochiometric equivalent of CO_3.

[c] TDS values are calculated based on Na and Ca + Mg estimated from the inverse model and their stochiometric equivalent of Cl and SO_4, respectively.

[d] Sum of the TDS derived from silicate, carbonate and evaporites weathering.

Table 4
Chemical weathering rates and CO_2 consumption for the Changjiang main channel

Sample	River, location	Surface area (10^4 km^2)	Water discharge (m^3/s)	SPM (mg/l)	Silicates				Carbonates			Evaporites	Total rock weathering
					Φsil (ton/km^2/year)	Cat sil[a] (10^6 ton/year)	Ca + Mg sil (10^9 mol/year)	CO_2 cons. (10^9 mol/year)	Φcarb (ton/km^2/year)	$TDS_{carb.}$[b] (10^6 ton/year)	CO_2 cons. (10^9 mol/year)	$TDS_{evap.}$[c] (10^6 ton/year)	TDS[d] (10^6 ton/year)
CJ-14	Changjiang, Chongqing	86.7	8,602	nd	1.7 ± 0.3	1.5 ± 0.3	18 ± 5	72 ± 13	9.6 ± 1.1	22 ± 1	233 ± 27	6 ± 1	29 ± 2
SX4	Changjiang, Yichang	100.6	8,894	4	2.3 ± 0.2	2.3 ± 0.2	26 ± 3	111 ± 9	10.1 ± 0.7	27.3 ± 0.7	286 ± 21	3.2 ± 0.7	33 ± 2
CJ-36	Changjiang, Datong	170.5	27,429	51	2.4 ± 0.5	4.1 ± 0.9	43 ± 16	191 ± 44	14 ± 3	62 ± 6	646 ± 155	7 ± 4	73 ± 10
CJ-52	Changjiang, Wuhan	148.8	19,761	54	3.3 ± 0.4	4.9 ± 0.6	55 ± 12	235 ± 32	13 ± 4	52 ± 6	543 ± 163	8 ± 2	65 ± 8
CJ-60	Changjiang, Yueyang	125	16,719	40	1.8 ± 0.2	2.3 ± 0.2	25 ± 3	109 ± 8	11 ± 0.8	37.4 ± 0.9	389 ± 26	4.5 ± 0.7	44 ± 2

The CO_2 consumption rates are based on the cationic contribution derived from the inverse model (see Appendix C). The incertitudes are estimated from the inverse model.

[a] The flux of cations derived from silicate weathering is related to the cationic weathering rate by Cat sil = Φsil × S where S stands for the surface area of the basin.

[b] TDS values are calculated based on the sum of the cations estimated from the inverse model and their stochiometric equivalent of CO_3.

[c] TDS values are calculated based on Na and Ca + Mg estimated from the inverse model and their stochiometric equivalent of Cl and SO_4, respectively.

[d] Sum of the TDS values dervived from silicate, carbonate and evaporites weathering.

Jialingjiang to 30 mm/kyr for the Minjiang and Xiangjiang. For the Changjiang Upper Reach, it reaches 13.5 mm/kyr (calculated at Chongqing, CJ14) in the same order of magnitude than that deduced from the Ganges–Brahmaputra system, 14–25 mm/kyr by Galy and France-Lanord (1999) for the western-central Nepal Himalaya. For the whole basin, the speed of chemical weathering averages 19 mm/kyr calculated at the Datong station.

As observed at the global scale (Gaillardet et al., 1999b) and at a more regional scale (Millot et al., 2003 for the Mackenzie basin), the main factor which seems to control the carbonates weathering is the runoff (Fig. 9a). As highlighted by these authors, this correlation rather reflects the greater variability of runoff from one sub-basin compared to the cationic TDS_{carb} (sum of Ca and Mg) than a real physical sense. In our study, the cationic TDS_{carb} is rather constant from one basin to another around 30 mg/l. It is interesting to note that the rates of silicates weathering does not obey to this law as reported in Millot et al. (2003). Several studies (Gaillardet et al., 1999b; Millot et al., 2002; Singh et al., 2005) have shown that the main parameter which controls the silicate weathering rate is the physical weathering rate. Estimation of this former parameter based on the SPM concentrations is source of uncertainties. At one sampling site, SPM concentration is not uniform in the river and

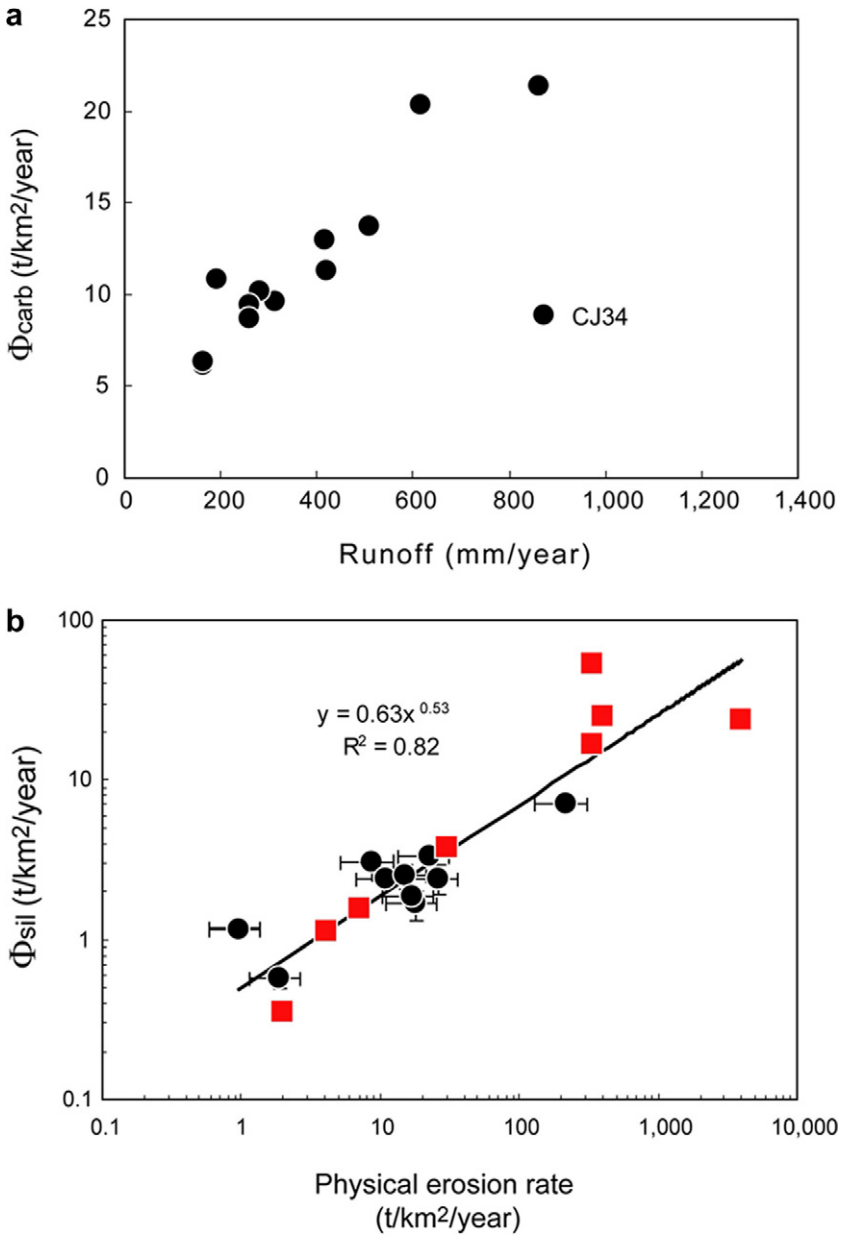

Fig. 9. Evolution of the cationic weathering rate of carbonates (Φ_{carb}) as a function of the runoff (a) and that of the cationic weathering rate of silicates (Φ_{sil}) as a function of the physical erosion rate (b). The full circles represent the rivers of the Changjiang basin (this study) with the exception of the sample collected at Yichang (SX4) and the squares, the data compiled in Millot et al. (2002).

should be integrated on depth profile. At sampling stations CJ36 and CJ52, we carried out two profiles to evaluate the change of the SPM concentration with depth. We observed changes of 40% and 20%, respectively, hence in the following discussion, we will ascribe an uncertainty of 40% to all the SPM concentrations. Another source of uncertainties is the effects of natural and artificial reservoirs on the storage of sediments that can lower the estimation of the physical weathering rates. This is a priori the case for the Changjiang and its tributaries for which a number of dams were built on their streams and partly explain the long-term reduction of the annual sediment discharge during the last decades (Yang et al., 2002; Chen et al., 2008). For 2006, the sediment discharge recorded at Datong falled to 85×10^6 tons compared to the 431×10^6 tons observed during the period 1953–1985 (Chen et al., 2008). Even so, because of the lack of data since the commencement of filling of the TGD (2003), it is not possible to distinguish the natural causes of this falling-off from the human disturbances.

Furthermore, whether the approach used to estimate the annual solute fluxes based on a single measurement and using the monthly average discharge value (so long as it is close to mean annual discharge) gives a reliable estimation (Qin et al., 2006) of these fluxes, the calculation of an annual physical erosion rate can be biased (Qin et al., 2006). Because the SPM are delivered by short pulses, it is crucial to sample this SPM flashes to have an accurate estimation of the annual physical denudation rates. We probably failed to sample this SPM peak as revealed by the difference between the annual SPM discharge calculated at Datong with the SPM concentration measured in this study and the monthly water discharge for August, 47×10^6 tons and the annual discharge of 85×10^6 tons reported by Chen et al. (2008) for the year 2006. Nevertheless, as both the chemical weathering fluxes and the physical erosion rates are calculated using the monthly discharges during the time of sampling and field data (SPM concentrations), this should not affect our comparison between the chemical weathering rates and the physical erosion.

We plotted in Fig. 9b the silicates weathering rates as a function of the physical weathering rates and compared with other studies compiled in Millot et al. (2002). Our results follow the same trend linking chemical and physical weathering rates established by Millot et al. (2002) and as reported by these authors and Gaillardet et al. (1999b) seems to be independent of the lithological variations.

5.5. Sources of protons as weathering agent and CO_2 consumption rates

As previously underlined, deciphering the sources of protons is crucial to estimate the CO_2 consumption by rocks weathering. In addition to CO_2, protons coming from sulphuric acid dissociation can increase the weathering rates and need to be taken into account for the weathering fluxes. Two main sources of sulphuric acid have to be considered, atmospheric inputs and sulphides oxidation. A part of the acids present in the atmosphere are neutralized in reaction involving soil dusts and ammonia as illustrated by the map of the acid rain deposition over China (Zhang et al., 2007). In Northern China and Tibetan Plateau, rains generally have a neutral or alkaline pH whereas the main acid rain depositions are observed for the Sichuan basin, the middle and lower parts of the Changjiang basin and the Southern China.

An evidence of the involvement of protons originating from H_2SO_4 is given by the Fig. 10a where we have plotted the DIC concentrations as a function of the cations released by silicate and carbonate weathering as derived from the inverse model and expressed in milliequivalents per liter. Our data deviate from the theoretical line 1:1, which is for chemical weathering reactions in the case where only CO_2 would be involved. A different way to present this result is to plot the same quantities as rates in equiv/km^2/year (Fig. 10b). In this diagram, we observe that the more intense the weathering rate is, more our data deviates from the line 1:1 and hence, weathering by H_2SO_4 is important and increases the carbonates and silicates weathering rate. Contribution from sulfuric acid to weathering reactions appears to be significant for the Wujiang and Minjiang. For the other samples, due to the propagated uncertainties, it is not possible to estimate accurately the contribution of H_2SO_4 in weathering reactions. Thus, for these samples, the calculated CO_2 consumption rates based on cationic contributions (Tables 3 and 4) will represent a maximum value. For the Minjiang and Wujiang, we can estimate based on the imbalance between the DIC concentrations and the sum of the cations derived from weathering of carbonates and silicates that around 220 and 500 μmol/l of H_2SO_4 were involved in chemical weathering reactions, respectively. Making the hypothesis that H_2SO_4 invloved in weathering reactions only reacts with carbonate rocks, we estimate that for the Minjiang, and the Wujiang contribution of H_2SO_4 weathering accounts for $37 \pm 11\%$ and $55 \pm 8\%$, respectively. The same observation was made by Han and Liu (2004) for the Wujiang who estimated a contribution of H_2SO_4 approaching 50%. This ensues to a carbonate weathering rate by sulphuric acid for the Wujiang of 21 ton/km^2/year close to the estimation based on sulfur isotopes, 35 ton/km^2/year, of Jiang et al. (2006) and 30 ton/km^2/year for the Minjiang. Thus, the CO_2 consumption rates by carbonate weathering and silicate weathering (see Appendix C) are respectively 35×10^9 and 45×10^9 mol/year for the Minjiang and 7.6×10^9 and 2.9×10^9 mol/year for the Wujiang. On the other hand, if H_2SO_4 only reacts with silicates (see Appendix C), the CO_2 consumption rates by carbonate weathering and silicate weathering are respectively 75×10^9 and 12×10^9 mol/year for the Minjiang and 13×10^9 and 0×10^9 mol/year for the Wujiang.

For the other tributaries, CO_2 consumption by silicate weathering varies from 7 to 8×10^9 mol/year for the Jialongjiang, Xiangjiang and Ganjiang to 18 to 19×10^9 mol/year for the Hanshui. As for CO_2 consumption by carbonate weathering, it is 2–7 times higher and ranges from 20×10^9 mol/year for the Ganjiang to 54×10^9 mol/year for the Xiangjiang.

Regarding the Changjiang main channel, we estimate CO_2 consumption by silicate weathering at Chongqing

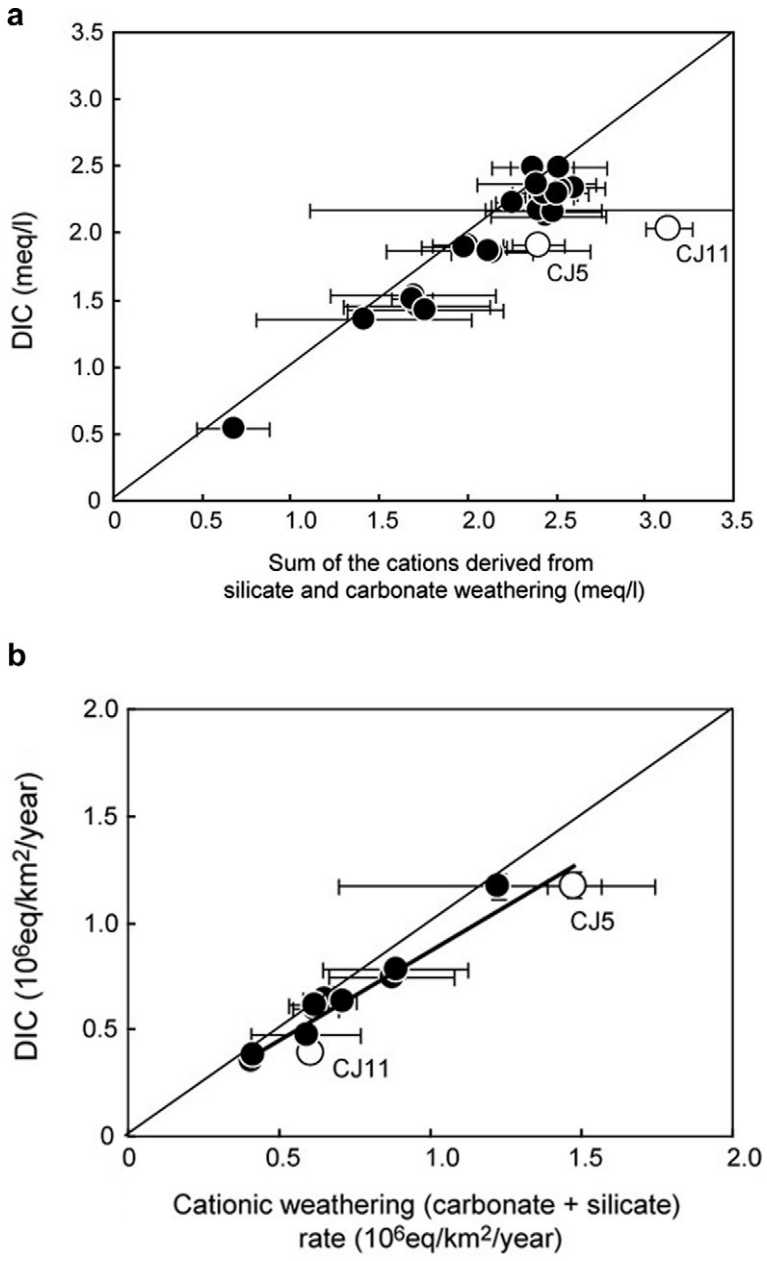

Fig. 10. DIC as a function of the sum of the cations derived from carbonates and silicates weathering (a) and DIC expressed in 10^6 equiv/km^2/year as a function of the cationic weathering rate of carbonates and silicates expressed in 10^6 equiv/km^2/year (b).

(CJ14) of 72×10^9 mol/year or 0.8×10^5 mol/km^2/year. This last value is similar to that deduced from other rivers draining the Tibetan Plateau, 0.7×10^5 mol/km^2/year (Singh et al., 2006) and 0.3–1.25×10^5 mol/km^2/year (Hren et al., 2007) as well as for the Upper Huang He, 0.9–1.2×10^5 mol/km^2/year (Wu et al., 2005). The estimation of the CO_2 consumption rates by carbonate weathering, 2.7×10^5 mol/km^2/year, is also comparable with the range of values reported in other studies for the Tibetan Plateau, 0.2–9×10^5 mol/km^2/year (Hren et al., 2007).

From our calculations, we estimate a consumption of CO_2 by carbonates and silicates weathering for the whole basin calculated at the Datong station of 646×10^9 mol/year (4×10^5 mol/km^2/year) and 191×10^9 mol/year (1×10^5 mol/km^2/year), respectively, and accounts for 5% and 2% of the global CO_2 consumption fluxes by carbonate and continental silicate rocks (Gaillardet et al., 1999b).

6. CONCLUSIONS

This geochemical study on the dissolved load of the Changjiang and its main tributaries showed that four major reservoirs (carbonates, silicates, evaporites and agriculture/urban effluents) contribute to the total dissolved solutes. In spite of its huge water discharge, the Changjiang reveals to be very sensitive to human activities. At the Datong station the contribution of anthropogenic inputs accounts for 15% of the cationic TDS. The riverine chemistry of the Changji-

ang basin is dominated by carbonates weathering, with a mean TDS_{carb} calculated at Datong of 62×10^6 ton/year. We conclude that the chemical weathering rates can be strongly enhanced by sulphuric acid dissociation derived from pyrite oxidation and atmospheric deposition. The CO_2 consumption for carbonate weathering reaches 646×10^9 mol/year at Datong whereas silicate weathering rates and CO_2 consumption flux are clearly lower, averaging 2.4 ton/km^2/year and 191×10^9 mol/year at Datong, respectively. The total chemical weathering rate (both silicates and carbonates) estimated for the Qinghai–Tibetan Plateau, calculated for the Upper Changjiang is 13.5 mm/kyr and for the whole basin reaches 19 mm/kyr calculated based on the water sample collected at Datong.

ACKNOWLEDGMENTS

The authors thank F.S. Wang, X.L. Liu, L.B. Li, H. Ding and J. Guan for their help during the samples collection as well as the staffs of the Datong and Wuhan hydrological stations. We also thank G.L. Han for her comments on a previous manuscript. W. Huang and S. Rothenberg are acknowledged for the English corrections and suggestions. Comments and suggestions by C. Dessert, S.K. Singh, E. Tipper and an anonymous reviewer greatly improved the quality of the manuscript. We are also grateful to S. Krishnaswami for his editorial handling and fruitful comments. This work was supported jointly by the Chinese Academy of Sciences through the International Partnership Project, by the National Natural Science Foundation of China (Grant No. 90610037) and by the Ministry of Science and Technology of China through the National Basic Research Program of China ("973" Program, Grant No. 2006CB4003200).

APPENDIX A. INVERSION MODEL

To solve the problem, we used a least square regression approach based on Na-normalized mass balance equations. A complete theory of inversion techniques is given in Tarantola (2005) and was successfully applied to river mass budgets (Negrel et al., 1993; Gaillardet et al., 1999b; Roy et al., 1999; Millot et al., 2003; Chetelat and Gaillardet, 2005). For each element X of interest (F, Na, Cl, NO_3, Ca, Mg, K and Sr), we can write a set of mass balance equations.

$$\left(\frac{X}{\mathrm{Na}}\right)_{\mathrm{river}} = \sum_{\mathrm{i}} \left(\frac{X}{\mathrm{Na}}\right)_{\mathrm{i}} \times \alpha_{\mathrm{i}}(\mathrm{Na})$$

And for the Sr isotopic composition, the mixing equation can be written as

$$\left(\frac{^{87}\mathrm{Sr}}{^{86}\mathrm{Sr}}\right)_{\mathrm{river}} \times \left(\frac{\mathrm{Sr}}{\mathrm{Na}}\right)_{\mathrm{river}} = \sum_{\mathrm{i}} \left(\frac{^{87}\mathrm{Sr}}{^{86}\mathrm{Sr}}\right)_{\mathrm{i}} \times \left(\frac{\mathrm{Sr}}{\mathrm{Na}}\right)_{\mathrm{i}} \times \alpha_{\mathrm{i}}(\mathrm{Na})$$

Where α_i(Na) represents the mixing proportion of Na from the different sources (i = atmosphere, agriculture, urban effluents, carbonate, silicate or evaporite).

In this approach, all the parameters are considered as unknown and are affected by error bars which reflect the knowledge of each parameter. The least known are the proportions of Na coming from the different sources. Then, the algorithm adjusts the different parameters from a set of *a priori* values by successive iterations that best fit the whole set of equations. This approach also allows to constrain the composition of poorly known end-member, i.e. agriculture in our case.

In our calculations, we assume that the $\left(\frac{X}{\mathrm{Na}}\right)_{\mathrm{river}}$ are known within 10% uncertainty and then, we estimated the different α_i(Na) with their error bars. The results show that the uncertainty on the different α_i(Na) is better than 10% for the agriculture, evaporite, carbonate and silicate sources whereas for the urban effluents and atmospheric sources it can reach 35%. For the calculation of the proportion of the other elements, the major source of uncertainties is the composition of the different end-members. The propagated errors for the different TDS are (in mean) 15% for the silicate and carbonate ones, 30% for the evaporites one and 35% for the anthropogenic (agriculture and urban effluents) and atmospheric ones.

To test the sensitivity of our inversion procedure, we used the Ca/Na and Mg/Na ratios of the silicate end-member reported in Qin et al. (2006) in the case of the Minjiang (CJ5). These two ratios, 0.7 and 0.3, respectively, are higher (especially the Ca/Na ratio) than those we used in our model (Table 2) and we proceeded to the calculation for the sample CJ5 by fixing the Ca/Na and Mg/Na ratios at the values reported in Qin et al. (2006) for the silicate endmembers, other *a priori* ratios being similar to those reported Table 2. Whereas the apportioned Mg to the different sources is similar between the two calculations (a maximum relative difference of 17% is observed for the apportioned Mg to silicate weathering), the amounts of Ca derived from the different sources present large relative differences between the two calculations up to 70% for the apportioned Ca to silicate weathering and anthropogenic inputs whereas the amounts appointed by other sources (atmosphere, carbonate and evaporites) are similar. The difference observed for the apportioned Ca to anthropogenic inputs results from the adjustment of the Ca/Na ratios for the urban end-member at a value much lower than that measured in the waste water samples and used as *a priori* parameter (Table appendix A). Regarding the cationic TDS, results show that the relative differences between the values calculated using our end-members and those of Qin et al. (2006) never exceed 20% with the exception of the cationic TDS derived from anthropogenic inputs which shows a relative difference of 40%.

Table appendix A
Elemental ratios adjusted by the model for the sensitivity test

	(Ca/Na)atm	(Ca/Na)urb	(Ca/Na)carb	(Ca/Na)sil	(Ca/Na)ev	(Mg/Na)atm	(Mg/Na)urb	(Mg/Na)carb	(Mg/Na)sil	(Mg/Na)ev
(1)	2.2	0.6	47	0.33	1.45	0.5	0.10	18	0.25	0.20
(2)	2.1	0.3	45	0.70	1.50	0.5	0.09	18	0.30	0.20

(1) This study and (2) the test by fixing the Ca/Na and Mg/Na ratios of the silicate end-member at the values reported in Qin et al. (2006).

APPENDIX B

Cationic TDS (mg/l) derived from the carbonate, silicate, evaporites, anthropogenic (agriculture and domestic/industrial waste water) and rainwater reservoirs calculated by the inversion model for the Changjiang main channel and its tributaries

	Sample	TDScarb.	σ	TDSsil. sil	σ	TDSevap.	σ	TDSanthro.	σ	TDSrain.	σ
Main channel											
	CJ1	33	4	10	1	37	2	0	0	1.1	0.6
	CJ3	33	3	10	1	17	1	0	0	1.4	0.5
	CJ4	38	3	9	1	12	1	0.3	0	1.1	0.5
	CJ6	33	1	12	1	7.9	0.7	5.1	0.6	2.4	0.3
	CJ7	32	16	12	1	6.4	0.5	11	1	1.8	0.3
	CJ10	31	3	7	1	5.3	0.9	14	3	1.3	1.0
	CJ13	28	3	9	1	7.5	0.4	18	1	2.1	0.9
	CJ14	31	4	5	1	6.8	0.9	18	4	1.9	0.5
	CJ12	36	4	6	1	5.8	0.9	14	2	1.4	0.7
	SX5	37	3	8	1	4.4	0.6	13	3	1.0	0.5
	SX4	36	3	8	1	4.2	0.7	13	3	2.2	0.6
	CJ60	27	3	4	1	2.9	0.4	11	1	1.9	0.4
	CJ52	31	9	8	1	4.1	0.7	7	2	3	2
	CJ44	26	7	5	1	4	1	7	3	5	3
	CJ36	27	6	5	1	3	1	7	3	5	3
	CJ41	28	7	5	1	3	1	9	3	4	3
Tributaries											
Yalongjiang	CJ2	34	2	6.8	0.2	0.6	0.1	0	0	1.1	0.4
Minjiang	CJ5	33	2	11.5	0.5	4	1	8	1	2.5	0.8
Jialingjiang	CJ9	38	3	7	1	6.6	0.9	9	1	1.7	0.4
Jialingjiang	CJ15	39	4	7	1	7	1	10	1	2.0	0.3
Wujiang	CJ11	52	2	3.6	0.2	1.3	0.4	6.9	0.6	4.4	0.6
Xiangjiang	CJ33	25	11	1.9	0.4	3	1	6	1	3	2
Ganjiang	CJ34	10	3	3.7	0.6	0	0	6	1	3.0	0.8
Hanshui	CJ46	37	4	9	1	7	3	9	3	3	2
Hanshui	CJ47	34	5	10	2	10	3	7	2	3	2

APPENDIX C

The first step in the calculation of silicate and carbonate weathering by carbonic acid is the estimation of the cations released by sulphuric acid weathering.

(1) Cations derived from weathering of carbonates and silicates by sulphuric acid:

- Weathering of carbonates by sulphuric acid:

$$2CaCO_3 + H_2SO_4 = 2Ca^{2+} + 2HCO_3^- + SO_4^{2-} \quad (1)$$

- Weathering of silicates by sulphuric acid:

For divalent-cation silicates:

$$CaAl_2Si_2O_8 + H_2SO_4 = Ca^{2+} + SO_4^{2-} + 2SiO_2 + 2AlOOH \quad (2)$$

For monovalent-cation silicates:

$$2NaAlSi_3O_8 + H_2SO_4 = 2Na^+ + SO_4^{2-} + 6SiO_2 + 2AlOOH \quad (3)$$

Hence, the amount of sulfuric acid consumed by carbonates weathering is calculated as:

$$SO_4carb = 0.5[Ca]carb + 0.5[Mg]carb \quad (4)$$

and the amount of sulfuric acid consumed by silicates weathering is calculated as:

$$SO_4sil = 0.5[Na]sil + 0.5[K]sil + [Ca]sil + [Mg]sil \quad (5)$$

According to Spence and Telmer (2005), the cations derived from silicates weathering by sulphuric acid can be deduced from Eq. (5) as:

$$Na^{SSW} = SO_4^{SSW} \times \left[\left(\frac{Ca}{Na}\right)_{sil} + \left(\frac{Mg}{Na}\right)_{sil} + 0.5\left(\frac{K}{Na}\right)_{sil} + 0.5\right]^{-1} \quad (6)$$

$$K^{SSW} = Na^{SSW} \times \left(\frac{K}{Na}\right)_{sil} \quad (7)$$

$$Ca^{SSW} = Na^{SSW} \times \left(\frac{Ca}{Na}\right)_{sil} \quad (8)$$

$$Mg^{SSW} = Na^{SSW} \times \left(\frac{Mg}{Na}\right)_{sil} \quad (9)$$

Where SSW stands for silicates weathering by sulphuric acid and $\left(\frac{X}{Na}\right)_{sil}$ (X = Ca, Mg and K) are the elemental ratios of the silicate end-member derived from the inverse model.

Thus for each element X (Na, K, Ca and Mg) derived from silicate weathering, the amount derived from weathering by carbonic acid (CSW) is calculated as:

$$X^{CSW} = Xsil - X^{SSW} \quad (10)$$

With Xsil the apportioned amount to silicate weathering derived from the inverse model.

A similar calculation can be done from Eq. (4) to estimate the cations derived from weathering of carbonates by sulphuric acid and carbonic acid (noted CCW)

(2) Cations derived from weathering of carbonates and silicates by carbonic acid:

- Weathering of carbonates by carbonic acid:

$$CaCO_3 + CO_2 + H_2O = Ca^{2+} + 2HCO_3^- \quad (11)$$

- Weathering of silicates by carbonic acid:

For monovalent-cation silicates

$$NaAlSi_3O_8 + CO_2 + 2H_2O = Na^+ + HCO_3^- + 3SiO_2 + Al(OH)_3 \quad (12)$$

For divalent-cation silicates

$$CaAl_2Si_2O_8 + 2CO_2 + 4H_2O = Ca^{2+} + 2HCO_3^- + 2SiO_2 + 2Al(OH)_3 \quad (13)$$

Hence, the amount of carbonic acid consumed by carbonates weathering is calculated as:

$$CO_2carb = Ca_{carb}^{CCW} + Mg_{carb}^{CCW} \quad (14)$$

and the amount of carbonic acid consumed by silicates weathering is calculated as:

$$CO_2sil = 2Ca_{sil}^{CSW} + 2Mg_{sil}^{CSW} + Na_{sil}^{CSW} + K_{sil}^{CSW} \quad (15)$$

We applied this formalism to estimate the CO_2 consumption by carbonate and silicate weathering for the Minjiang and Wujiang in the simplified cases where either sulphuric acid only reacts with carbonates or only reacts with silicates. The amount of H_2SO_4 involved in weathering reactions was estimated based on the imbalance observed between the measured DIC concentrations and the sum of the cations derived from carbonate and silicate weathering.

In the case of the Wujiang, if we assume that H_2SO_4 only reacts with silicates, the protons are in excess that leads to a consumption of CO_2 by silicate weathering of 0. Thus, the excess H_2SO_4 calculated as $H_2SO_4^{excess} = H_2SO_4 - (0.5[Na]sil + 0.5[K]sil + [Ca]sil + [Mg]sil)$ reacts with carbonates as discussed above.

REFERENCES

Aas W., Shao M., Jin L., Larssen T., Zhao D., Xiang R., Zhang J., Xiao J. and Duan L. (2007) Air concentrations and wet deposition of major inorganic ions at five non-urban sites in China, 2001–2003. *Atmos. Environ.* **41**, 1706–1716.

Berner R. A., Lassaga A. C. and Garrels R. M. (1983) The carbonate-silicate geochemical cycle and its effect on atmospheric carbon-dioxide over the past 100 million years. *Am. J. Sci.* **283**, 641–683.

Bickle M. J., Chapman H. J., Bunbury J., Harris N. B. W., Fairchild I. J., Ahmad T. and Pomies C. (2005) Relative contributions of silicate and carbonate rocks to riverine Sr fluxes in the headwaters of the Ganges. *Geochim. Cosmochim. Acta* **69**(9), 2221–2240.

Blum J. D. and Erel Y. (1997) Rb–Sr isotope systematics of a granitic soil chronosequence: the importance of biotite weathering. *Geochim. Cosmochim. Acta* **61**(15), 3193–3204.

Calmels D., Gaillardet J., Brenot A. and France-Lanord C. (2007) Sustained sulfide oxidation by physical erosion processes in the Mackenzie River basin: climatic perspectives. *Geology* **35**(11), 1003–1006.

Chen Z., Li J., Shen H. and Wang Z. (2001) Yangtze River of China: historical analysis of discharge variability and sediment flux. *Geomorphology* **41**, 77–91.

Chen J., Wang F., Xia X. and Zhang L. (2002) Major element chemistry of the Changjiang (Yangtze River). *Chem. Geol.* **187**(3–4), 231–255.

Chen X., Yan Y., Fu R., Dou X. and Zhang E. (2008) Sediment transport from the Yangtze River, China, into the sea over the Post-Three Gorge Dam Period: a discussion. *Quat. Int.* **186**(1), 55–64.

Chetelat B. and Gaillardet J. (2005) Boron isotopes in the Seine River, France: a probe of anthropogenic contamination. *Environ. Sci. Technol.* **39**(8), 2486–2493.

Dalai T. K., Krishnaswami S. and Sarin M. M. (2002) Major ion chemistry in the headwaters of the Yamuna river system: chemical weathering, its temperature dependence and CO_2 consumption in the Himalaya. *Geochim. Cosmochim. Acta* **66**(19), 3397–3416.

Dessert C., Dupre B., Gaillardet J., Francois L. M. and Allegre C. J. (2003) Basalt weathering laws and the impact of basalt weathering on the global carbon cycle. *Chem. Geol.* **202**(3–4), 257–273.

Ding T., Wan D., Wang C. and Zhang F. (2004) Silicon isotope compositions of dissolved silicon and suspended matter in the Yangtze River, China. *Geochim. Cosmochim. Acta* **68**(2), 205–216.

Dosseto A., Bourdon B. and Turner S. P. (2008) Uranium-series isotopes in river materials: insights into the timescales of erosion and sediment transport. *Earth Planet. Sci. Lett.* **265**(1–2), 1–17.

Flintrop C., Hohlmann B., Jasper T., Korte C., Podlaha O. G., Scheele S. and Veizer J. (1996) Anatomy of pollution; rivers of North Rhine–Westphalia, Germany. *Am. J. Sci.* **296**(1), 58–98.

Fu B.-J., Zhuang X.-L., Jiang G.-B., Shi J.-B. and Lü Y-H. (2007) Environmental problems and challenges in China. *Environ. Sci. Technol.* **41**, 7597–7602.

Gaillardet J., Dupre B. and Allegre C. J. (1999a) Geochemistry of large river suspended sediments: silicate weathering or recycling tracer? *Geochim. Cosmochim. Acta* **63**(23–24), 4037–4051.

Gaillardet J., Dupre B., Louvat P. and Allegre C. J. (1999b) Global silicate weathering and CO_2 consumption rates deduced from the chemistry of large rivers. *Chem. Geol.* **159**(1–4), 3–30.

Galy A. and France-Lanord C. (1999) Weathering processes in the Ganges-Brahmaputra basin and the riverine alkalinity budget. *Chem. Geol.* **159**, 31–60.

Gerard F., Mayer K. U., Hodson M. J. and Ranger J. (2008) Modelling the biogeochemical cycle of silicon in soils: Application to a temperate forest ecosystem. *Geochim. Cosmochim. Acta* **72**(3), 741–758.

Godderis Y., Donnadieu Y., Nedelec A., Dupre B., Dessert C., Grard A., Ramstein G. and Francois L. M. (2003) The Sturtian 'snowball' glaciation: fire and ice. *Earth Planet. Sci. Lett.* **211**(1–2), 1–12.

Godderis Y. and Francois L. M. (1995) The Cenozoic evolution of the strontium and carbon cycles: relative importance of

continental erosion and mantle exchanges. *Chem. Geol.* **126**(2), 169–190.

Han G. and Liu C.-Q. (2004) Water geochemistry controlled by carbonate dissolution: a study of the river waters draining karst-dominated terrain, Guizhou Province, China. *Chem. Geol.* **204**(1–2), 1–21.

Han G. and Liu C.-Q. (2006) Strontium isotope and major ion chemistry of the rainwaters from Guiyang, Guizhou Province, China. *Sci. Total Environ.* **364**(1–3), 165–174.

Hren M. T., Chamberlain C. P., Hilley G. E., Blisniuk P. M. and Bookhagen B. (2007) Major ion chemistry of the Yarlung Tsangpo–Brahmaputra river: Chemical weathering, erosion, and CO_2 consumption in the southern Tibetan plateau and eastern syntaxis of the Himalaya. *Geochim. Cosmochim. Acta* **71**(12), 2907–2935.

Huh Y., Tsoi M.-Y., Zaitsev A. and Edmond J. M. (1998) The fluvial geochemistry of the rivers of Eastern Siberia. I: tributaries of the Lena River draining the sedimentary platform of the Siberian Craton. *Geochim. Cosmochim. Acta* **62**(10), 1657–1676.

Jacobson A. D., Blum J. D. and Walter L. M. (2002) Reconciling the elemental and Sr isotope composition of Himalayan weathering fluxes: insights from the carbonate geochemistry of stream waters. *Geochim. Cosmochim. Acta* **66**(19), 3417–3429.

Jiang Y.-K., Liu C.-Q. and Tao F.-X. (2006) The role of sulfur cycling in carbonate weathering: isotope geochemistry of sulfur in the Wujiang River catchment, Southwest China. *Chinese J. Geochem.* **25**, 278.

Lang Y.-C., Liu C.-Q., Zhao Z.-Q., Li S.-L. and Han G.-L. (2006) Geochemistry of surface and ground water in Guiyang, China: water/rock interaction and pollution in a karst hydrological system. *Appl. Geochem.* **21**(6), 887–903.

Larssen T., Seip H. M., Semb A., Mulder J., Muniz I. P., Vogt R. D., Lydersen E., Angell V., Dagang T. and Eilertsen O. (1999) Acid deposition and its effects in China: an overview. *Environ. Sci. Policy* **2**(1), 9–24.

Lebron I. and Suarez D. L. (1996) Calcite nucleation and precipitation kinetics as affected by dissolved organic matter at 25 °C and pH > 7.5. *Geochim. Cosmochim. Acta* **60**(15), 2765–2776.

Li M., Xu K., Watanabe M. and Chen Z. (2007) Long-term variations in dissolved silicate, nitrogen, and phosphorus flux from the Yangtze River into the East China Sea and impacts on estuarine ecosystem. *Estuar. Coast. Shelf Sci.* **71**, 3–12.

Liu S. M., Zhang J., Chen H. T., Wu Y., Xiang H. and Zhang Z. F. (2003) Nutrients in the Changjiang and its tributaries. *Biogeochemistry* **62**, 1–18.

Liu C.-Q., Masuda A., Okada A., Yabuki S. and Fan Z.-L. (1994) Isotope geochemistry of Quaternary deposits from the arid lands in northern China. *Earth Planet. Sci. Lett.* **127**(1–4), 25–38.

Liu C. Q., Li S. L., Lang Y. C. and Xiao H. Y. (2006) Using $\delta^{15}N$ and $\delta^{18}O$ values to identify nitrate sources in karst ground water, Guiyang, Southwest China. *Environ. Sci. Technol.* **40**, 6928–6933.

Luo L., Qin B., Song Y. and Yang L. (2007) Seasonal and regional variations in precipitation chemistry in the Lake Taihu Basin, China. *Atmos. Environ.* **41**(12), 2674–2679.

Meybeck M. (1986) Composition des ruisseaux non pollues de France. *Sci. Geol. Bull.* **39**, 3–77.

Millot R., Gaillardet J., Dupre B. and Allegre C. J. (2002) The global control of silicate weathering rates and the coupling with physical erosion: new insights from rivers of the Canadian Shield. *Earth Planet. Sci. Lett.* **196**(1–2), 83–98.

Millot R., Gaillardet J., Dupre B. and Allegre C. J. (2003) Northern latitude chemical weathering rates: clues from the Mackenzie River Basin, Canada. *Geochim. Cosmochim. Acta* **67**(7), 1305–1329.

Moon S., Huh Y., Qin J. and van Pho N. (2007) Chemical weathering in the Hong (Red) River basin: rates of silicate weathering and their controlling factors. *Geochim. Cosmochim. Acta* **71**(6), 1411–1430.

Negrel P., Allegre C. J., Dupre B. and Lewin E. (1993) Erosion sources determined by inversion of major and trace element ratios and strontium isotopic ratios in river: the Congo Basin case. *Earth Planet. Sci. Lett.* **120**(1–2), 59–76.

Oliver L., Harris N., Bickle M., Chapman H., Dise N. and Horstwood M. (2003) Silicate weathering rates decoupled from the $^{87}Sr/^{86}Sr$ ratio of the dissolved load during Himalayan erosion. *Chem. Geol.* **201**(1–2), 119–139.

Qin J., Huh Y., Edmond J. M., Du G. and Ran J. (2006) Chemical and physical weathering in the Min Jiang, a headwater tributary of the Yangtze River. *Chem. Geol.* **227**(1-2), 53–69.

Raymo M. E., Ruddiman W. F. and Froelich P. N. (1988) Influence of late Cenozoic mountain building on ocean geochemical cycles. *Geology* **16**, 649–653.

Roy S., Gaillardet J., Dupré B. and Allègre C.-J. (1996) Strontium Isotope Geochemistry of the Largest Rivers of China. Implication for Weathering Rates. Goldschmidt Conference, Heidelberg.

Roy S., Gaillardet J. and Allegre C. J. (1999) Geochemistry of dissolved and suspended loads of the Seine River, France: anthropogenic impact, carbonate and silicate weathering. *Geochim. Cosmochim. Acta* **63**(9), 1277–1292.

Singh S. K., Kumar A. and France-Lanord C. (2006) Sr and $^{87}Sr/^{86}Sr$ in waters and sediments of the Brahmaputra river system: silicate weathering, CO_2 consumption and Sr flux. *Chem. Geol.* **234**(3–4), 308–320.

Singh S. K., Sarin M. M. and France-Lanord C. (2005) Chemical erosion in the eastern Himalaya: major ion composition of the Brahmaputra and $[\delta]^{13}C$ of dissolved inorganic carbon. *Geochim. Cosmochim. Acta* **69**(14), 3573–3588.

Spence J. and Telmer K. (2005) The role of sulfur in chemical weathering and atmospheric CO_2 fluxes: evidence from major ions, $\delta^{13}CDIC$, and $\delta^{34}SSO_4$ in rivers of the Canadian Cordillera. *Geochim. Cosmochim. Acta* **69**(23), 5441–5458.

Stallard R. F. and Edmond J. M. (1981) Geochemistry of the Amazon. Precipitation chemistry and the marine contribution to the dissolved load at the time of the peak discharge. *J. Geophys. Res.* **86**, 9844–9858.

Tipper E. T., Galy A. and Bickle M. J. (2006) Riverine evidence for a fractionated reservoir of Ca and Mg on the continents: implications for the oceanic Ca cycle. *Earth Planet. Sci. Lett.* **247**(3–4), 267–279.

Tarantola A. (2005) *Inverse problem theory and methods for model parameter estimation*. SIAM, Philadelphia.

Tu J., Wan H., Zhang Z., Jin X. and Li W. (2005) Trends in chemical composition of precipitation in Nanjing, China, during 1992–2003. *Atmos. Res.* **73**(3–4), 283–298.

Viers J., Dupré B., Deberdt S., Braun J. J., Angeletti B., Ndam Ngoupayou J. and Michard A. (2000) Major and traces elements abundances, and strontium isotopes in the Nyong basin rivers (Cameroon): constraints on chemical weathering processes and elements transport mechanisms in humid tropical environments. *Chem. Geol.* **169**, 211–241.

Wang Y.-X., Yang J.-D., Chen J., Zhang K.-J. and Rao W.-B. (2007a) The Sr and Nd isotopic variations of the Chinese Loess Plateau during the past 7 Ma: implications for the East Asian

winter monsoon and source areas of loess. *Palaeogeogr. Palaeoclimatol. Palaeoecol.* **249**(3–4), 351–361.

Wang Z.-L., Zhang J. and Liu C.-Q. (2007b) Strontium isotopic compositions of dissolved and suspended loads from the main channel of the Yangtze River. *Chemosphere* **69**(7), 1081–1088.

Wu L., Huh Y., Qin J., Du G. and van Der Lee S. (2005) Chemical weathering in the Upper Huang He (Yellow River) draining the eastern Qinghai–Tibet Plateau. *Geochim. Cosmochim. Acta* **69**(22), 5279–5294.

Xing G. X. and Zhu Z. L. (2002) Regional nitrogen budgets for China and its major watersheds. *Biogeochemistry*(57/58), 405–427.

Xu Z. and Liu C.-Q. (2007) Chemical weathering in the upper reaches of Xijiang River draining the Yunnan–Guizhou Plateau, Southwest China. *Chem. Geol.* **239**, 83–95.

Xue L., Fu J. C., Wang F. Y. and Wang L. Q. (2005) A mixture model approach to analyzing major element chemistry data of the Changjiang (Yangtze River). *Environmetrics* **16**(3), 305–318.

Yang S.-L., Zhao Q.-Y. and Belkin I. M. (2002) Temporal variation in the sediment load of the Yangtze river and the influences of human activities. *J. Hydrol.* **263**, 56–71.

Zeng X.-Z. and Sun J. (1999) The actuality of organic fertilizer input into arable land and the measure to develop soil fertility in Zunyi Prefecture. *Cult. Plant.* **5**, 59–60, (in Chinese).

Zhang J., Ren J. L., Liu S. M., Zhang Z. F., Wu Y., Xiong H. and Chen H. T. (2003) Dissolved aluminum and silica in the Changjiang (Yangtze River): impact of weathering in subcontinental scale. *Global Biogeochem. Cycles* **17**(3), 1–11.

Zhang M., Wang S., Wu F., Yuan X. and Zhang Y. (2007) Chemical compositions of wet precipitation and anthropogenic influences at a developing urban site in southeastern China. *Atmos. Res.* **84**, 311–322.

Associate editor: S. Krishnaswami